Journal of Holography Applications in Physics
Volume 2, Issue 3, Summer 2022, 1-54

DOI:10.22128/jhap.2022.540.1025

Journal of Holography Applications in Physics

Review article

Review on Top-Down Kondo-like Holographic RG Flows

Christian Northe
Institut für Theoretische Physik und Astrophysik,
Julius-Maximilians-Universität Würzburg, Am Hubland, 97074 Würzburg, Germany.
Würzburg-Dresden Cluster of Excellence ct.qmat,
Julius-Maximilians-Universität Würzburg, Am Hubland, 97074 Würzburg, Germany;
email: christian.northe@physik.uni-wuerzburg.de

Received: June 06, 2022; Accepted: July 13, 2022.

Abstract. The Kondo model, i.e. the screening of magnetic impurities in a metal, has been a pillar of theoretical physics ever since its first establishment in 1964. This article provides an introduction to a recent top-down realization of the Kondo effect within the framework of the AdS/CFT correspondence, which appeared in [1,2]. These sources describe an entire class of Kondo-like renormalization group flows, based on (p,q)-string impurities embedded into $AdS_3 \times S^3 \times M_4$, which all mimic the brane condensation description of the Kondo effect. In order to provide a lucid introduction, this review only discusses the simplest case of pure D1-brane impurities inside the F1/NS5 brane system. Choosing a stack of D1-branes occupying an AdS_2 sheet within AdS_3 and localized to a point on the S^3 as UV configuration, the flow has the D1-branes puff up into D3-branes wrapping stably an S^2 in the IR, whose polar angle on S^3 is determined by the D1-brane charge of the system. This setup allows to describe the case where the impurity is exactly screened, just as in the original Kondo effect. Moreover, the g-factors are computed and shown to decrease along the flow, thereby confirming the validity of the g-theorem for this class of flows. This holographic model of the Kondo effect has two virtues. First, its ambient CFT is not only known, but also well studied. Second, the flow preserves the maximal amount of supersymmetry, i.e. four supercharges; these are enhanced to eight superconformal charges at the fixed points.

Keywords: AdS/CFT Correspondence; Interfaces; Boundaries; RG Flows; Impurities; Supergravity.

Contents

1 Introduction

Boundaries, defects and interfaces are amongst the most natural things occurring in nature. Any experiment in the laboratory, in particular, is bounded in extent and hence requires an understanding of edge effects. Defects and interfaces, furthermore, appear as domain walls, separating different regions of space and time. If these regions are governed by the same theory, we speak of defects and if this is not the case, we speak more generally of interfaces. Defects and interfaces appear naturally, say in the Ising model, or in low-dimensional systems as impurities, as is relevant in this article. A powerful formalism, malleable enough to be any of the three aforementioned possibilities, is that of Dirichlet branes (D-branes), which arises from string theory and is very important in the following. In a nutshell, in this review, we model impurities in gravitational setups via Dirichlet branes, and thereafter, we study their behavior under a change of energy scale.

To become more concrete, it pays off to begin with the prototypical example in which thy physics of impurities is studied at low temperatures, namely the Kondo effect [3]. Kondo's model couples free electrons to a spin-1/2 impurity via spin-spin interaction. Upon lowering the temperature, this setup displays an anomalous logarithmic growth in resistivity, precisely as observed experimentally in doped metals. This was a huge breakthrough! On the one hand, experimentalists had been yearning for an explanation of their observations for over thirty years. On the other hand, theory would come to profit a lot from the existence of Kondo's description in 1964 until today.

Most significantly, Kondo's setup was instrumental in the development of the renormalization group (RG) [4]. In this framework, the impurity was captured by the RG flow of a defect. Importantly, the model has a negative beta function, indicating a non-trivial IR fixed point even though the UV fixed point is so simple. At low temperatures, the impurities form bound states with conduction electrons. This has two effects. First, the impurities are screened, leading to a change in boundary condition implemented at the defect. Second, the bound electrons no longer contribute to the conductivity, hence the rise in resistivity.

Ever since 1964, the Kondo model has become a pillar of theoretical physics, serving as toy model in various arenas. Besides the aforementioned RG procedure, the Kondo model earned its merits in the testing of techniques such as Fermi liquids [5], the Bethe Ansatz [6, 7] and large-N limits [8]. More relevant for this review are the incentives that the Kondo model gave for advancing our understanding of boundary conformal field theory (BCFT) [9–19] and of defect conformal field theory [20, 21]. Even today, Kondo physics has not fallen out of fashion. Contemporary research, amongst many others, is concerned with *nanotechnology* [22] and *quantum dots* [23, 24].

A complementary study of the Kondo model within the framework of the anti-de Sitter/conformal field theory (AdS/CFT) correspondence holds a number of perks. First, both the simplicity and the applicability of Kondo's model make it an excellent prototype for the study of more complicated holographic defects and interfaces. A few well-known and recent examples are studied in [25–31]. Second, its importance means that any new generalizations or techniques provided by holography may lead to new insights, as has occurred in the study of QFT. Third, the free electron gas itself is replaced by a strongly coupled system. This is particularly important, since strongly coupled systems are notoriously hard to control, and remarkably, within the AdS/CFT correspondence, strongly coupled QFTs are described elegantly via weakly coupled gravity theories.

Holographic versions of the Kondo model have already been considered. First in [32], and later, in a series of papers [33–40], a holographic dual of the entire RG flow between UV and IR fixed points was established. This model is motivated by a top-down brane construction, where a D3-brane background is supplemented by D5- and D7-brane probes.

The D3-D5 brane and D3-D7 brane systems are separately supersymmetric. However, the combination of D5- and D7-brane probes breaks supersymmetry, giving rise to a tachyon potential inducing the Kondo flow.

Unfortunately, the dual gravity action of this system remains unknown. Hence, a bottom-up model incorporating the primary characteristics of the top-down model was brought forth in [33]. It gave rise to a number of remarkable results. First, the screening of the impurity is realized geometrically in the gravity theory as decrease in flux, proportional to the number of defect degrees of freedom, through the boundary of AdS_2. As appropriate for an impurity in a strongly coupled system [41], the resistivity depends polynomially on temperature, with real exponent, rather than the $\log T$ behavior of the original Kondo model. Moreover, two-point functions and Fano resonances were computed in this setup [38,39], it was possible to extract the impurity's entropy, including its backreaction on its surroundings [36], quenches of the Kondo coupling were described [40] and even the case of two defects was investigated [35].

In spite of these successes, it is desirable to construct a top-down model that improves on the shortcomings in the model described above. Therefore, a new model, which is the object of this review, was constructed in [1]. Compared to its predecessor, this new model possesses the following remarkable properties: its field theory description is accessible, it possesses non-chiral fermions making up the electron gas, and it has a parameter corresponding roughly to a number of electron "flavors". Finally, and most important for quantitative comparisons between the gravitational and field theoretic descriptions, it preserves a fraction of supersymmetry along the RG flow.

The inspiration for the model in [1] derives from the D-brane picture of the Kondo model [14, 42], which describes the screening of a Kondo impurity via the Myers effect [43] on $SU(2) \simeq S^3$: a stack of D0-branes, representing the UV impurity, condenses into a single D2-brane in the IR.

The most natural choice of ambient model, in which this brane condensation is implemented, is the D1/D5 system. It has two virtues. First, it is the best-studied example of AdS_2/CFT_3 holography and, in particular, the Lagrangian of the ambient CFT is known. Second, and more importantly, the type IIB superstring dual lives on $AdS_3 \times S^3 \times M_4$, the S^3 subfactor therein being the natural arena to stage the brane condensation of the Kondo flow. The impurities in this model are always interfaces rather than defects, and they are realized in the gravitational dual by adding p fundamental strings preserving half of the supersymmetries of the ambient D1/D5 CFT.

The CFT arises on the Higgs branch of a D1/D5 gauge theory compactified on a compact Calabi-Yau 4-manifold M_4 [44]. On the Higgs branch, the D1-branes are dissolved into the D5-branes thereby becoming gauge instantons on M_4. The gauge theory Lagrangian of the interface itself lends itself to the ADHM construction [45] via the Wilson line operator constructed in [46]. This ascribes a natural connection on the target space of the CFT to each point of M_4. This connection naturally induces an interface joining distinct D1/D5 CFTs. These interfaces have a natural generalization in which the fundamental strings are replaced by (p, q)-string bound states.

Turning to the gravity side, these interfaces are realized by (p, q)-strings, which intersect the D1/D5 system or end on it.

In the probe brane approximation, the near horizon geometry of the holographic dual is $AdS_3 \times S^3 \times M^4$, and the (p, q)-strings lie on an AdS_2 slice inside AdS_3 and are localized to a point in $S^3 \times M^4$. As shown in [1] and recapitulated in this review, these interfaces possess a marginally relevant operator, whose RG flow preserves four supersymmetries. Just as in the original Kondo model [47, 48], after deforming by this operator, the brane locus inside S^3 puffs up via the Myers effect from a point into an S^2. The RG scale in this setup is naturally given by the radial coordinate of AdS_3.

The probe brane setup is the tool of choice if one is interested only in the leading interaction between the interface and the CFT. However, in order to access effects of the interface on CFT observables, gravitational backreaction of the interface on its surroundings has to be considered. The next step is therefore to construct a backreacted supergravity dual to the interface flow. In fact, this task is too ambitious. However, it is possible to find the backreacted supergravity interface solutions dual only to the fixed points. The way to derive the desired solutions is through the general ansatz of asymptotically $AdS_3 \times S^3 \times M^4$ solutions to IIB supergravity of [49]. The class of geometries we seek, is found by relaxing the regularity conditions employed there.

In contrast to the probe brane description, where the F1 charge p of the interface is bound to remain macroscopically small compared to the background's D1 and D5 charge in order not to abandon the approximation, p can be dialed up all the way to the order of the D5 charge in the backreacted solutions. In particular, when p equals the D5 charge the D3 has slid down from the north to the south pole of the S^3 and the interface vanishes. This is the exact analog of the original Kondo flow, i.e. when only a single flavor of electrons and a spin-1/2 impurity is present. This is referred to as "critical" or "exact" screening. When this occurs, the spin of the conduction electrons has formed an SU(2) singlet with the spin of the impurity. Physically, the conduction electrons absorb the impurity.

The number of degrees of freedom on the interface is measured by the so-called g-factor or boundary entropy [50], which was shown to not increase along the flow from the UV to the IR [51, 52]. This is the celebrated g-theorem.

The boundary entropy can be extracted from the entanglement entropy [53], which in turn is computed to leading order in $1/c$ by the Ryu-Takayanagi prescription [54] in holography. This can be molded into a prescription to compute the interface entropy [55] at the fixed points of the RG flow. Finally, it can be confirmed that these results abide by the g-theorem.

It is the subject of this review to explain in detail the gravity side of this holographic Kondo flow, which appeared in [1, 2]. The philosophy follows closely that of [1], however, to add some additional substance, we put a slight spin on the material presented there. Namely, all computations are presented in the F1/NS5 frame rather than the D1/D5 frame. Extensive elaborations on the material presented here, in particular the F1/NS5 frame, which divert from the main train of thought, can be found in [2]. In this review, the field theory is not discussed, as it is mostly still under investigation; interested readers are referred to [1].

This review is organized as follows. In section 2, we begin with an introduction to the Kondo effect. Its description in terms of field theory, conformal field theory and as brane condensation process are discussed. Then, in section 2.3, the holographic implementation of the Kondo flow as condensation process in the probe brane approximation is presented. This proceeds in two steps. First, we show that a marginally relevant perturbation exists in the UV. Second, we describe the tripped flow and show that it has a non-trivial IR fixed point. In section 4, fully backreacted supergravity solutions are presented, first for the pure F1/NS5 geometry and building on that the geometries for the UV and IR fixed points. The latter two solutions are then related to each other by the RG flow. Over-screening and critical screening are discussed. Finally, in section 5 boundary entropies are computed and shown to decrease along the flow, i.e. the validity of the g-theorem is verified. What follows are conclusions and a compilation of outstanding problems in section 6. Appendices on boundary CFT and interface CFT section A and page charges accompany appendix B are meant to help novices find their way into the topic.

2 The Kondo Effect

Heavy magnetic impurities are screened in metals by conduction electrons at low temperatures. This is the essence of the Kondo effect [3]. Its description in terms of a quantum field theory is characterized by a negative beta function, signalling that the IR theory is non-trivial even though the UV theory is trivial. This feature turns the Kondo model into a toy model for quantum chromodynamics. More importantly for this review, the Kondo effect is the first example of an interface RG flow in theoretical physics.

Given a conducting material, as the temperature decreases, one of two scenarios can arise:

1. The resistivity decreases monotonically until a finite non-zero value is reached, as depicted in yellow in figure 1.

2. The system enters a superconducting phase at some critical temperature, and the resistivity vanishes, as shown in green in figure 1.

A third possibility was observed by experimentalists in the 1930s in the case that the material was doped with impurities. Here, an anomalous increase in resistivity emerged when the temperature was lowered sufficiently. It took until 1964 for theory to deliver an explanation [3]. The Japanese physicist Jun Kondo realized that this increase is caused by spin-spin interactions of conduction electrons with heavy magnetic spin impurities. At high energies, the impurities are ignored by the electrons, but in the IR the impurities become the center of attention for the electrons:

3. At low energies, the magnetic impurities form bound states with the conduction electrons, thereby screening the impurity; see figure 2. In consequence, new contributions to scattering arise, leading to an increase in resistivity. This is drawn in blue in figure 1.

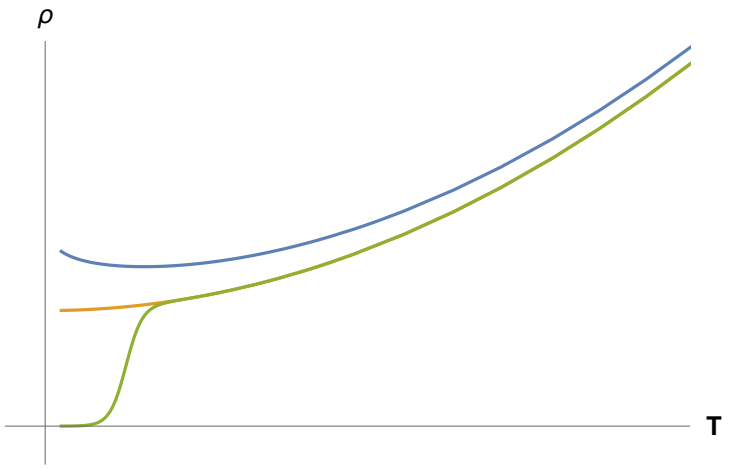

Figure 1: Resistivities against temperature for (1) normal conducting material drawn in yellow, (2) superconducting material drawn in green, (3) conductor with impurity drawn in blue. This sketch appears with permission of C. Melby-Thompson and has appeared before in [2]. (For interpretation of the references to color in this figure legend, the reader is referred to the web version of this article.)

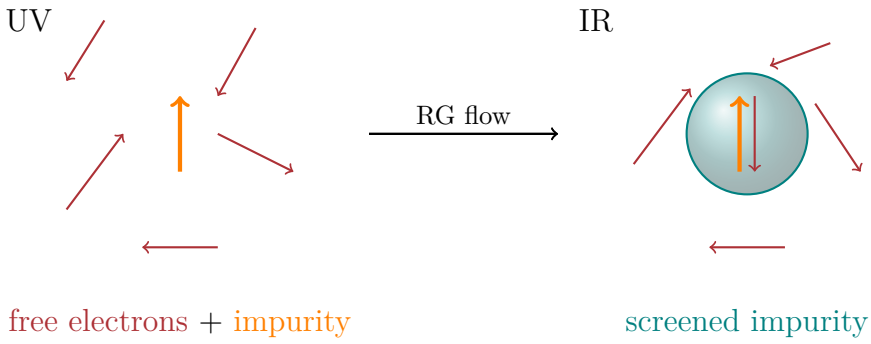

Figure 2: UV: Free electrons and uncoupled impurity. IR: Conduction electrons screen the impurity by forming a bound state with the impurity. In the original Kondo problem only a single electron couples to the impurity. When multiple channels are at play, more than one electron may couple to the impurity. This figure is adapted from [2]. (For interpretation of the references to color in this figure legend, the reader is referred to the web version of this article.)

Ever since 1964, the Kondo model has accompanied theoretical physics, serving as toy model in various areas. To name a few, it was central in the development of Wilson's renormalization group (RG) [4], and it presents fertile ground for techniques such as Fermi liquids [5], the Bethe Ansatz [6, 7] and large-N limits [8]. More relevant for this review are the incentives that the Kondo model gave in furthering our understanding of boundary conformal field theory (BCFT) [9–19] and of defect conformal field theory [20, 21]. Finally, versions of the Kondo model have been investigated in holography. First in [32], and later, in a series of papers [33–40], a holographic dual of the entire RG flow linking the UV and IR fixed points was established. Other contemporary activity dealing with the Kondo model is concerned with *nanotechnology* [22] and *quantum dots* [23, 24], amongst others.

2.1 Field Theory Review of the Kondo Effect

This section introduces the standard description of the Kondo effect within the framework of field theory following closely [2, 33, 56]. The setting is that of free electrons of mass m in $(3+1)$-dimensions coupled to an impurity $\vec{S}$,

$$H_K = \psi^\dagger_\alpha \frac{-\nabla^2}{2m}\psi_\alpha + \hat{\lambda}\delta(\vec{r})\vec{S}\cdot\psi^\dagger_{\alpha'}\frac{1}{2}\vec{\sigma}_{\alpha'\alpha}\psi_\alpha \tag{2.1}$$

The fermionic modes $\psi^\dagger_\alpha$ and ψ_α assume values in the fundamental representation of SU(2), corresponding to spin-up, $\alpha = \uparrow$, or spin down, $\alpha = \downarrow$. The impurity $\vec{S}$, localized at the origin by the δ-distribution, is also valued in the fundamental representation of SU(2). The generators in the fundamental of $\mathfrak{su}(2)$ are chosen to be given by the Pauli-matrix three-vector $\vec{\sigma}$. The coupling is ferromagnetic if $\hat{\lambda} < 0$ and anti-ferromagnetic if $\hat{\lambda} > 0$.

The Kondo effect is revealed on mathematical grounds by an RG flow, which describes the decrease in temperature. Therefore, it is necessary to contemplate the beta function of $\hat{\lambda}$. To leading order in perturbation it is negative. This means that for $\hat{\lambda} < 0$, the effective coupling vanishes at low energies, rendering the theory trivial. On the other hand, if $\hat{\lambda} > 0$ interesting physics arises at low energies. Namely, a dynamically generated scale emerges,

i.e. the *Kondo temperature* T_K. This property is called asymptotic freedom. Interestingly, the effective coupling appears to diverge at low energies, giving rise to the Kondo problem:

$$\text{What is the ground state of the Kondo Hamiltonian (2.1)?} \tag{2.2}$$

A heuristic answer is as follows. At short wavelengths, the system consists of free electrons and a decoupled spin. By lowering the temperature, the system is driven to longer wavelengths until the Kondo temperature T_K is reached. At this point, a single electron forms an SU(2) singlet with the impurity $\vec{S}$, thereby screening it and triggering a change of ground state. Hence, the impurity appears to be absent at low energies and the remaining electrons form a Landau Fermi liquid around it. The impurity is not exactly gone, though. It survives as boundary condition on the unbound electrons of the fermi liquid, forcing their wave functions to vanish at the locus of the bound state. This configuration is the new ground state. Physically, the electrons cannot enter the immediate surroundings of the bound state since this requires overcoming the binding energy proportional to $\hat{\lambda} \gg 1$, which is highly improbable. This process is depicted in figure 2.

The issue of a diverging coupling constant $\hat{\lambda}$ is also cleared up by the change up ground state. The coupling constant appears divergent if looked at from the point of view of the UV theory, not, however, in the IR theory, where the degrees of freedom have rearranged into free electrons supplemented by a special boundary condition. Ergo, nothing dramatic is going on.

The impurities of interest in our holographic setup are not valued in SU(2), but rather in representations of SU(N) with large N. Therefore, our mathematical description of the heuristic picture above is directly carried out for SU(N). Moreover, multiple flavors[1] k of electrons are incorporated. This enhances the symmetry group of the theory to

$$\mathrm{SU}(N) \times \mathrm{SU}(k) \times \mathrm{U}(1), \tag{2.3}$$

where SU(k) is the channel symmetry. The charge symmetry U(1) is already present for a single flavor. The electrons are now valued in the fundamental representation of SU(N) $\times$ SU(k). It is important to note that the impurity is in a finite dimensional representation of SU(N), i.e. it neither notices the SU(k) factor nor the charge symmetry $U(1)$. It transforms as a singlet under SU(k) $\times$ U(1). A Kondo system is then characterized by N, k and the representation of the impurity. The original Kondo problem treats conventional spin, $N = 2$, and has only a single flavor, $k = 1$, while the impurity is valued in the spin $\mathtt{s} = 1/2$ representation of SU(2).

2.2 Kondo Model as CFT

The Kondo effect has been described in many guises over the years. Most useful to our needs is its phrasing as a (1+1)-dimensional system pioneered by Affleck and Ludwig [9–13]. They observed that the only contributions to electronic scattering, were s-wave modes, so that only the radial distance r from the impurity is of importance. This mirrors in the fact that the impurity term proportional to $\delta(x)$ in (2.1) is spherically symmetric about the origin. Furthermore, the Kondo effect is already captured at energies close to the Fermi surface, so that it is legitimate to linearize the dispersion relation of the system around the Fermi momentum k_F. What remains is a description of the Kondo model using only a single spatial dimension, r. The out- and in-going s-waves are represented by right- and left-moving fermions, respectively. These fermions are not independent, being connected to each other by the impurity, which imposes a boundary condition, $\psi_L|_{r=0} = \psi_R|_{r=0}$. This is depicted in the LHS of figure 3.

[1] Condensed matter physicists refer to a flavor as a channel.

Figure 3: The Kondo model as $(1+1)$-dimensional system. On the left panel we have left- and right-moving fermions moving toward and away from the impurity and communicating via a boundary condition set by the impurity. On the right, after unfolding, only right moving fermions remain. The impurity presents no longer a boundary, but a defect. This figure is adapted from [2]. (For interpretation of the references to color in this figure legend, the reader is referred to the web version of this article [https://jhap.du.ac.ir/].)

This description is in terms of a boundary field theory. Via the "inverse" of the folding trick discussed in appendix A, the *unfolding trick*, this system is viewed as two chiral fermion field theories connected through an interface. Concretely, the right-movers are reflected about the origin, thereby becoming left-movers. This extends the radial direction to negative values. What remains are left-moving s-wave fermions, which propagate toward the impurity, communicate with it and move past it. In this review, the boundary theory is distinguished from the interface theory by the label of the spatial coordinate. While in the boundary theory it is called r, in the interface theory it is x. This is depicted on the RHS of figure 3. The coupling of the left-moving fermions to the impurity interface is described by the Hamiltonian

$$H = \frac{v_F}{2\pi}\psi_L^\dagger i\partial_x\psi_L + v_F\lambda\delta(x)\vec{S}\cdot\psi_L^\dagger\frac{\vec{\sigma}}{2}\psi_L, \tag{2.4}$$

where $v_F = k_F/m$ is the Fermi velocity and the $SU(N)$ indices have been suppressed on the fermions. Note that $\vec{\sigma}$ is now a vector containing the generators of $\mathfrak{su}(N)$ in their fundamental representation. The coupling λ is related to the coupling in (2.1) via $\lambda = \frac{k_F^2}{2\pi^2 v_F}\hat{\lambda}$. As customary in the CFT literature, the characteristic velocity of the system is fixed to be $v_F = 1$. Because $\delta(x)$ and $\vec{S}$ have dimension zero, while ψ_L has dimension one-half, the Kondo coupling is classically marginal.

The Kondo Model and CFT

Clearly the problem simplifies after reducing its dimensionality, since the differential operator in (2.1) reduces from ∇ to ∂_x in (2.4). But this by itself is in fact not the real advantage of cutting down two dimensions. The real reason is that (2.4) exhibits an infinite amount of symmetry, which is lacking in (2.1). Indeed, conformal symmetry emerges, and in fact it is even extended to affine $\hat{\mathfrak{su}}(2)_1$. When studying generalized Kondo impurities with k channels, corresponding to the symmetry group (2.3), this algebra is enhanced to

$$\hat{\mathfrak{su}}(N)_k \times \hat{\mathfrak{su}}(k)_N \times \hat{\mathfrak{u}}(1). \tag{2.5}$$

This enormous amount of emergent symmetry allows to determine the entire IR spectrum of the Kondo problem very elegantly, thereby answering an extension of the question (2.2).

Using complex coordinates $z = t + ix$, the currents generating the SU(N) factor in the symmetry algebra (2.5) are constructed from the fermions by

$$J^a(z) = \left(\psi^{\alpha,i}(T^a)_\alpha{}^\beta\psi_{\beta,i}\right)(z) = \sum_{n\in\mathbb{Z}} z^{n-1}J_n^a. \tag{2.6}$$

T^a is a generator of SU(N), hence $a = 1, \dots N^2 - 1$, and it is represented in the fundamental of SU(N), meaning that α, β run (as before) from 1 to N. The index i is in the fundamental of SU(k), i.e. $i = 1, \dots, k$. The modes of these currents obey an $\hat{\mathfrak{su}}(N)_k$ Kac-Moody algebra[2],

$$\left[J^a_n, J^b_m\right] = if^{abc}J^c_{n+m} + k\frac{n}{2}\delta^{ab}\delta_{n,-m}. \tag{2.7}$$

Here, f^{abc} are the structure constants of SU(N).

A set of currents analogous to (2.6) is employed for $\hat{\mathfrak{su}}(k)_N$

$$J^A(z) = \left(\psi^{\alpha,i}(T^A)_i{}^j\psi_{\alpha,j}\right)(z) = \sum_{n\in\mathbb{Z}} z^{n-1}J^A_n, \tag{2.8}$$

where T^A is a generator of SU(k) so that $A = 1, \dots, k^2 - 1$. The modes of these currents furnish an $\hat{\mathfrak{su}}(k)_N$ algebra, i.e. the algebra (2.7) with k replaced by N and a, b replaced by A, B. The structure constants f^{ABC} appearing here are those of SU(k).

Last but not least, the algebra $\hat{\mathfrak{u}}(1)$ has only a single current

$$J(z) = \left(\psi^{\alpha,i}\psi_{\alpha,i}\right)(z) = \sum_{n\in\mathbb{Z}} z^{n-1}J_n. \tag{2.9}$$

The $\hat{\mathfrak{u}}(1)$ currents obey, as well, a version of (2.7). Since U(1) has only one generator, the structure constants vanish. Equivalently, one can argue that they must vanish since U(1) is abelian. In consequence, only with the last term proportional to the level remains. By rescaling the modes J_n the level can be removed in the case of $\hat{\mathfrak{u}}(1)$[3]. What remains is the *Heisenberg algebra*,

$$[J_n, J_m] = \frac{n}{2}\delta_{n,-m}. \tag{2.10}$$

The Spectrum

Having assigned the symmetry algebra of this system, it is possible to answer the question of how many ground states there are. These follow from integrable representations of the affine algebra [57,58]. It suffices to consider the factor $\hat{\mathfrak{su}}(N)_k$. Its ground states are in one-to-one correspondence with the WZW primaries of the theory. There are $k+1$ such primaries, and they are labelled by their spin $0, \frac{1}{2}, \dots, \frac{k}{2}$. For $\hat{\mathfrak{su}}(k)_N$ the story is identical with k replaced by N. Of course the remaining part of the algebra (2.5) assigns additional information to the ground states of $\hat{\mathfrak{su}}(N)_k$, however, it is not important at present. The representations of $\hat{\mathfrak{u}}(1)$ become important later on when matching boundary conditions below in the context of the Kondo flow.

Now that the ground states are at hand, the spectrum is easily constructed using the modes J^a_n, J^A_n, J_n with $n > 0$. This is the usual Fock space construction, up to the subtlety of null vectors, which we gloss over here.

2.2.1 Absorption of Boundary Spin

We are now in a position to assign mathematical meaning to the heuristic explanation of the Kondo effect presented in figure 2. Rather than employing the (2.4), in CFT it is favorable to

[2]Note that we have chosen a slightly different normalization here than in the appendix (A.5). The normalization here is more in tune with spin, reflected in a factor of two in the second summand of the RHS.

[3]Note that rescaling the modes in the non-abelian case, rescales the structure constants. Thus this process is not without consequence.

perform the analysis in terms of the energy-momentum tensor following from the Sugawara construction and coupling the impurity,

$$T = \frac{1}{2\pi(N+k)} J^a J^a + \frac{1}{2\pi(k+N)} J^A J^A + \frac{1}{4\pi N k} J^2 + \lambda\delta(x)\vec{S}\cdot\vec{J}. \tag{2.11}$$

One of its advantages over (2.4) is that the spin, channel and charge degrees of freedom can be treated separately. By introducing a new current

$$\mathcal{J}^a \equiv J^a + \pi(N+k)\lambda\delta(x)S^a. \tag{2.12}$$

the energy momentum tensor may be brought into the form

$$T = \frac{1}{2\pi(N+k)} \mathcal{J}^a \mathcal{J}^a + \frac{1}{2\pi(k+N)} J^A J^A + \frac{1}{4\pi N k} J^2, \tag{2.13}$$

after completing the square and dropping a constant term $\propto \vec{S}\cdot\vec{S}$. This energy-momentum tensor already takes the form of the Sugawara construction. However, this is deceiving. but does it truly correspond to a Kac-Moody algebra (2.7)? In fact, (2.13) only corresponds to a Kac-Moody algebra (2.7) when the coupling assumes the special non-zero value

$$\lambda = \frac{2}{N+k}. \tag{2.14}$$

Together, (2.13) and (2.14) represent the IR fixed point of the RG flow [56]. This is the mathematical description of the absorption of impurity spin explained heuristically in figure 2. We already discussed that the impurity is remembered by the fermions through the IR boundary condition at the origin. Furthermore, the implications for the spectrum can also be investigated, starting from the observation that the symmetry algebra of the theory is again (2.5). Hence, the states are necessarily organized in representations of the same type as before. Importantly, they are not the same as in the UV.

The circumstance that the impurity spin is valued in a representation of $\mathfrak{su}(N)$ – the finite-dimensional restriction of $\hat{\mathfrak{su}}(N)_k$ – inspired Affleck and Ludwig to propose the following description of the Kondo flow [56]: Only the representations of $\hat{\mathfrak{su}}(N)_k$ undergo the RG flow, while the representations of $\hat{\mathfrak{su}}(k)_N$ are just spectators. The RG flow itself is realized through *fusion*[4] between the ground states of the UV theory and the representation of the impurity. The fusion rules of $\hat{su}(2)_k$, for instance, are

$$N_{j_1 j_2}^{j_3} = \begin{cases} 1 & \text{if } |j_1 - j_2| \leq j_3 \leq \min(j_1+j_2, k-j_1-j_2) \text{ and } j_1+j_2+j_3 \in \mathbb{Z}, \\ 0 & \text{otherwise.} \end{cases} \tag{2.15}$$

To illustrate the rearrangement of representations due to the Kondo flow, we consider the simplest example: the original Kondo problem which has $N = 2$, $k = 1$ and $\mathsf{s} = 1/2$. There is no flavor symmetry factor, because there is only one flavor. We start with the ground state of spin $j_1 = 0$, and we fuse the impurity spin $j_2 = \mathsf{s} = 1/2$ onto it. Inspecting (2.15), this gives $j_3 = 1/2$ as the only possible fusion product. Similarly, if we choose the other ground state, $j_1 = 1/2$, and fuse $j_2 = \mathsf{s} = 1/2$ onto it, we find $j_3 = 0$. In other words, all that happens under the RG flow is that the two ground states are interchanged.

How can we detect that the representations have indeed been interchanged? The answer lies, in the remaining symmetries which in the case at hand is just the charge symmetry $U(1)$. In the UV all states build on the spin $j = 0$ ground state have odd $U(1)$ charge, while those build on the spin $j = 1/2$ ground state have even $U(1)$ charge. Importantly, the $U(1)$ charges remain fixed under the RG flow. Therefore, after interchanging the representations the $j = 0$ states have even $U(1)$ charge, while the $j = 1/2$ states have odd $U(1)$ charge.

[4] We provide a brief introduction to the fusion rules of a CFT in appendix A.1.2

2.2.2 Types of Screening

When more than one electron flavor is available, $k > 1$, three distinct types of screening arise, depending on the impurity spin s [48]:

Critical screening occurs when $k = 2\mathsf{s}$. Sufficient electron flavors are present in the system to screen the impurity completely. The IR physics is that of k free left-movers and no impurity. This happens by default in the original Kondo problem.

Over-screening occurs when $k > 2\mathsf{s}$. The system contains too many electron flavors, all trying to screen the impurity. The resulting bound state develops negative effective spin, which requires new screening by the surrounding electrons in the fermi liquid. This process continues, giving rise to multiple layers surrounding the impurity.

Under-screening occurs when $k < 2\mathsf{s}$. The system does not contain enough flavors to screen the impurity completely. The IR physics is described by k free left-movers and an impurity of reduced spin $|\mathsf{s} - k/2|$.

In the holographic description of the Kondo effect of this review, we will only encounter the first two scenarios.

2.3 Kondo RG flow as Brane Condensation

While the field theory description of the Kondo effect delivered up until here is well known, it is not the description we wish to adapt in holography. Rather we turn to a lesser known, yet very powerful way of thinking about the Kondo effect pioneered two decades ago by the CFT community [14–19]. It rephrases the Kondo effect as a condensation process between branes, thereby introducing the picture of the Kondo effect that we aim to mimic in holography: A stack of D-particles situated on the north-pole of a three-sphere condenses into a single two-sphere at fixed polar angle on said three-sphere.

In this subsection, we provide a minimal introduction to the method; a detailed account of is found in [59]. To keep the discussion short here, we have chosen to write this subsection for readers familiar with conformally invariant boundary conditions of the model $\hat{\mathfrak{su}}(2)_k$. All readers unfamiliar with this construction need not worry, however, as we provide a lightning review to the ingredients in appendix A. The explicit CFT details are in fact not so important to understand our holographic construction later on. Yet, the picture to be explained here, figure 4, is the main take-away of section 2, as it lies at the heart of all that follows.

The advertised picture arises from a rule which is generally applicable to boundary RG flows in CFT, and it indicates how boundary conditions change in dependence of the perturbing operator. This rule is called the “absorption of boundary spin" principle. We state the rule [11, 14, 59] and thereafter explain it with an application.

Given an impurity $\vec{S}$ valued in the spin-s irreducible representation of SU(2), the characters transform under an RG flow according to

$$(2\mathsf{s}+1)\chi_j(\tau) \xrightarrow{RG} \sum_l N^l_{j\mathsf{s}}\,\chi_l(\tau) \tag{2.16}$$

where s is the impurity spin, $(2\mathsf{s}+1)$ is the dimension of the SU(2) representation of spin s, $\chi_j(\tau)$ is the character of the $\hat{\mathfrak{su}}(2)_k$ representation $\mathcal{H}_j$ and N^k_{ij} are the fusion rules of $\hat{\mathfrak{su}}(2)_k$. All these concepts are introduced in section A.

In words, the rule states (2.16) the following: A fixed number, determined by the impurity spin s, of representations $\mathcal{H}_j$ in the UV BCFT reshuffle under an RG flow according to the

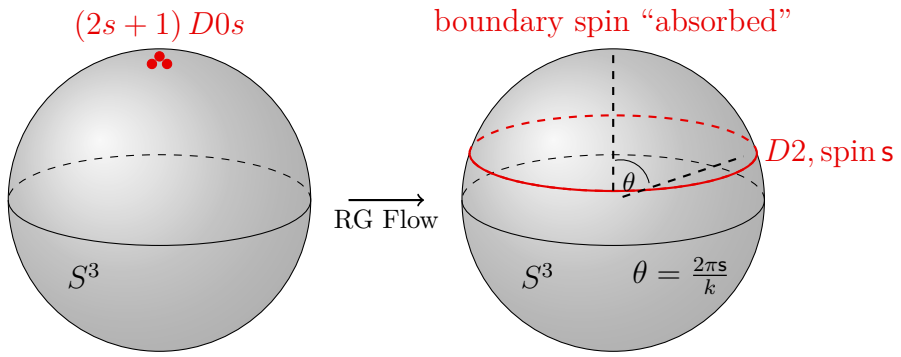

Figure 4: A stack of $(2\mathsf{s}+1)$ D0 branes condense into a single brane of spin s at fixed polar angle $\theta = 2\pi\mathsf{s}/k$. This process describes the absorption of an impurity by surrounding electrons in the Kondo model. This figure appeared before in [1, 2]. (For interpretation of the references to color in this figure legend, the reader is referred to the web version of this article [https://jhap.du.ac.ir/].)

fusion rules of the impurity spin s and the representation $\mathcal{H}_j$ at hand. The fusion rules relevant in the Kondo model are those of $\hat{\mathfrak{su}}(2)_k$, eq. (2.15).

The rule (2.16) might seem abstract, but it is in fact very simple to apply. Consider the partition function of a single brane of spin j in the $\hat{\mathfrak{su}}(2)_k$ model[5],

$$Z_j(\tau) = \sum_{i=0}^{k/2} N_{jj}^i \, \chi_i(\tau). \tag{2.17}$$

When considering a stack of M branes, it is important to keep in mind that the end of each open string may be attached to any of the M branes. As a result, the partition function of the stack of M branes is M^2 times the partition function of the single brane,

$$Z_{(M,\,j)} = M^2 \, Z_{(1,\,j)} = M^2 \sum_{l=0}^{k/2} N_{j\,j}^l \, \chi_l(\tau). \tag{2.18}$$

The first subscript indicates the amount of stacked branes, while the second subscript labels the branes' type, here spin j. Important in the Kondo model is a stack of $M_\mathsf{s} = (2\mathsf{s}+1)$ pointlike branes ($D0$-branes) located at the north pole, that is, branes of spin $j = 0$, with spectrum

$$Z_{(M_\mathsf{s},\,0)} = M_\mathsf{s}^2 \, Z_{(1,\,0)} = M_\mathsf{s}^2 \, \chi_0(\tau) \tag{2.19}$$

which uses $N_{00}^l = \delta_0{}^l$. To implement an RG flow, the "absorption of boundary spin" principle (2.16), has to be applied once for each end of the open string, i.e. twice,

$$\begin{aligned} Z_{(M_\mathsf{s},\,0)} &= M_\mathsf{s}^2 \, \chi_0(\tau) \\ &\longrightarrow M_\mathsf{s} \, \chi_\mathsf{s}(\tau) \\ &\longrightarrow \sum_l N_{\mathsf{s}\,\mathsf{s}}^l \, \chi_l(\tau) = Z_{(1,\,\mathsf{s})}. \end{aligned} \tag{2.20}$$

[5] This partition function is derived in section A.2.

This is indeed the result obtained originally by Affleck and Ludwig [9] and the rule (2.16) recovers it without breaking a sweat. The stack of pointlike branes $D0$-branes of spin $j = 0$ has decayed into a *single* brane of spin $j = \mathsf{s}!$ When $2\mathsf{s} < k$, i.e. overscreening, we obtain spherical $D2$-brane wrapping the S^3 at constant polar angle $\theta = 2\pi\mathsf{s}/k$. When $2\mathsf{s} = k$, i.e. exact screening, the decayed brane is again pointlike and sits at the south pole $\theta = \pi$. This process is called a brane condensation, and it is illustrated in figure 4.

The objective of this article is to review how this picture of the Kondo effect is implemented in holography using a full string theory construction [1].

3 A Kondo Condensation in Holography

After this extensive introduction to the Kondo effect, and in particular to its description in terms of a brane condensation, it is time to turn to its realization in holography. Put plainly, we seek an implementation of figure 4 in holography. That this is possible has been demonstrated in [1] for a large class of holographic interfaces, which assume the role of the Kondo impurity. An extensive description of this work is found in [2].

Sticking with two-dimensional CFT, the obvious environment for our Kondo model is type IIB string theory on $\mathrm{AdS}_3 \times \mathrm{S}^3 \times T^4$. This geometry has the benefit of naturally incorporating a three-sphere, on which a version of figure 4 can be staged. A stronger hint for the suitability of this geometry is found when realizing this geometry as near-horizon limit of the F1/NS5 system. In this case, the S^3 factor has a description as a $\hat{\mathfrak{su}}(2)_k$ WZW model, just as the Kondo model.

A remarkable feature of the flows we describe is that they preserve supersymmetry along the flow. In order for this to be possible, the brane configuration is not just purely situated on the three-sphere, but is also extended on the AdS_3 part [60]. In both, the UV and IR, the extension into AdS_3 assumes the shape of an AdS_2 slice, securing an $SO(2,1)$'s worth of isometries. This matches the symmetries of a $(0+1)$ dimensional conformal defect theory. Precisely what is desired!

Choosing the F1/NS5 frame, the flows described in [1, 2] start out in the UV with a stack of (p, q) strings, which are AdS_2 slices inside AdS_3 and dots on the S^3. Concretely, these interfaces are p D1-branes with q fundamental strings attached. In the IR this stack of branes has condensed into a single D3-brane charged under the one-brane charges of the UV configuration,

$$\text{UV: } p\ D1_q(\mathrm{AdS}_2) \qquad \longrightarrow \qquad \text{IR: } 1\ D3_{p,q}(\mathrm{AdS}_2 \times \mathrm{S}^2). \tag{3.1}$$

The parentheses indicate the geometry of the brane's worldvolume. The AdS_2 slice indicates that both configurations preserve the conformal group in $(0+1)$ dimensions, i.e. $\mathrm{SO}(2,1)$, as appropriate for an interface CFT in two dimensions. Furthermore, both configurations preserve an $\mathrm{SU}(2)$, as appropriate for a Kondo impurity. On top of this, both configurations are 1/2-BPS, that is, out of the 16 superconformal charges in the near-horizon limit of the F1/NS5 system 8 are preserved at the fixed points. While conformality is lost along the flow, still 4 supersymmetries persist, giving an analytic handle for the flow's description.

It turns out that these impurities are always interfaces, never defects, meaning that the CFTs connected by the impurity are never the same theory. The D1 charge causes the electric field to differ in the ambient CFTs, while the F1 charge even shifts their central charges. In this review, for the sake of clarity, we only describe the simplest impurity out of this broader class, namely that of p "pure" D1-branes, without any number of fundamental strings attached, $q = 0$,

$$\text{UV: } p\ D1\,(\mathrm{AdS}_2) \qquad \longrightarrow \qquad \text{IR: } 1\ D3_p(\mathrm{AdS}_2 \times \mathrm{S}^2), \tag{3.2}$$

where the subscript on the D3 indicates that p units of D1-brane charge are dissolved on the D3-brane. Readers, interested in impurities with $q \neq 0$, may take this review as a stepping stone to understand the article [1]. Readers, who are new to the subject may even consult [2], which is aimed at novices.

The flow, and thus our description of it, falls into two parts. The first concerns the LHS of (3.2), in which a stack of D1-branes begins to decay. Using the non-abelian DBI action, we demonstrate in section 3.2 that such a flow is indeed triggered. Once the flow is tripped, the question remains whether the flow has a non-trivial fixed point. This is the subject of section 3.3, in which we show that the configuration stabilizes on the S^3 at a fixed polar angle determined by the amount D1-brane charge in the UV.

3.1 AdS_2-Branes and S^2-branes

This subsection collects the results of [60] on AdS_2-branes inside AdS_3, and the results of [61] on S^2-branes inside S^3. For explicit derivations, the reader may consult the original sources. For a very pedestrian tutorial also [2] may be consulted.

3.1.1 AdS_2-Branes

Choosing Poincar patch coordinates on AdS_3

$$ds^2 = L^2 \frac{dz^2 - dt^2 + dx^2}{z^2} \tag{3.3}$$

where L is the AdS radius. The Kalb-Ramond two-form is

$$B = -\frac{L^2}{z^2} dt \wedge dx \qquad \Rightarrow \qquad \hat{B} = \frac{L^2}{z^2} x' dz \wedge dt. \tag{3.4}$$

In this section, pullbacks to the worldvolume of the brane are denoted by hats. The solution to the abelian DBI action without F1 charge, $q = 0$ in the notation above is

$$A_t = a, \qquad x(z) = x_0 = \text{const.} \tag{3.5}$$

Since the gauge field is constant, the gauge field strength vanishes[6]

$$F_{zt} = \partial_z A_t = 0 \tag{3.6}$$

Since x has no z dependence, the AdS_2-brane fall orthogonally to the boundary into the bulk of AdS_3. This is depicted in figure 5. As an aside, turning on F1 charge q, the x-coordinate of the brane acquires a linear z-dependence, so that it falls into the bulk at an angle [60].

Note that plugging the solution (3.5) into (3.4) yields $\hat{B} = 0$. Combining this with the solution for F, the gauge invariant field strength becomes

$$\mathcal{F} = \hat{B} + 2\pi\alpha' F = 0 \tag{3.7}$$

3.1.2 S^2-Branes

Choosing spherical coordinates on S^3,

$$ds^2 = L^2 \left[d\theta^2 + \sin^2\theta (d\phi^2 + \sin^2\phi \, d\chi^2) \right]. \tag{3.8}$$

[6] The gauge $A_z = 0$ was employed in the derivation.

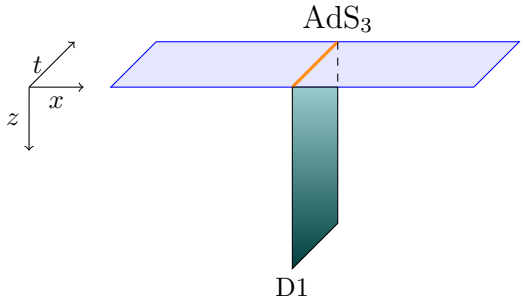

Figure 5: A D1 interface (shaded in teal) hangs down orthogonally to the boundary into AdS. In the CFT the interface is just the orange line, which splits the CFT spacetime (blue) in half. Two distinct CFTs are found to either side. This figure is adapted from [2]. (For interpretation of the references to color in this figure legend, the reader is referred to the web version of this article.)

When combining this spherical brane with the AdS_2 brane above, by supersymmetry the sphere radius is forced to coincide with the AdS radius. Using string data this is

$$L^2 = k\alpha' \,. \tag{3.9}$$

The Kalb-Ramond two-form is

$$B = L^2\big(\theta - \sin\theta\cos\theta\big)\,\omega_{S^2} = L^2\big(\theta - \sin\theta\cos\theta\big)\,\sin\phi\, d\phi \wedge d\chi. \tag{3.10}$$

The gauge field strength is

$$F = -\frac{p}{2}\,\omega_{S^2} \qquad \Leftrightarrow \qquad \int_{S^2} F = -2\pi p. \tag{3.11}$$

where p is a D-particle charge responsible for the stabilization of the brane at fixed polar angle

$$\theta_p := \frac{\pi\alpha' p}{L^2} \overset{(3.9)}{=} \frac{\pi p}{k} \tag{3.12}$$

This angle is a local minimum of the energy and it maintains this interpretation in the supersymmetric combinations of section 3.3. In fact, in that case, the charge p counts the D1-branes hanging into AdS_3. Observe that for $\theta_p = 0$ or $\theta_p = \pi$, the brane is pointlike, while if it is in between those values it is an S^2. This is similar to the discussion in section A.2.2.

Finally, the flux coming from the gauge invariant combination

$$\mathcal{F} = \hat{B} + 2\pi\alpha' F = L^2\big(\theta - \sin\theta\cos\theta - \theta_p\big)\omega_{S^2} \tag{3.13}$$

is not quantized.

3.2 Non-abelian brane polarization

The subject of this subsection is to investigate the vicinity of the UV fixed point, in which the impurity is given by a stack of p $D1$-branes. That is, we investigate the l.h.s. of (3.2). The proper framework to study such a setup is that of the non-abelian DBI action [43]. A review, which introduces our notation, is found in section 2.1.2 of [2]. The main objective

is to derive the dimension of the perturbing operator and show that it is relevant, so that the perturbing operator indeed drives the system out of the UV fixed point. In fact, we find that the operator is marginally relevant, just as in the original Kondo problem.

For our purposes, it will be sufficient to evaluate this non-abelian DBI action to cubic order in the polar angle field θ on the S^3. Again, we consider only the case of vanishing F-string charge on the interface. In this setup however this does not affect the result, since our considerations are entirely independent of the F-string charge, i.e. the results here are the same for any kind of (p,q)-string interface.

Because the S^3 factor has a description in terms of an $\hat{\mathfrak{su}}(2)_k$ WZW model in the F1/NS5 system, which is employed here, it is no surprise that a natural deformation of the type described in section 2.3 exists in our holographic setup. An important difference is that the string worldsheet theory in the presence of a deformation remains conformal, so that the RG flow in the WZW model is now realized as a "dynamical" process evolving in the direction of increasing z. The perturbing operator in the CFT is dual to the polar angle field θ in the gravity theory. For our purposes, it suffices to evaluate the non-abelian DBI action to cubic order in θ in order to extract its scaling dimension.

In order to investigate what happens when the flow starts, it is convenient to work with stereographic coordinates on S^3:

$$ds^2_{S^3} = \frac{(2\,d\vec{y})^2}{(1+r^2)^2}\,, \qquad \vec{y}\in\mathbb{R}^3\,, \tag{3.14}$$

which relate to polar coordinates via $r=\tan\frac{\theta}{2}$. In stereographic coordinates the NS two-form B on S^3 assumes the form

$$B_{S^3} = \ell^2 b\,\omega_{S^2} = \ell^2 b\frac{\epsilon_{ijk}y^i dy^j\wedge dy^k}{r^3}\,, \tag{3.15}$$

$$b = \theta - \sin\theta\cos\theta\,. \tag{3.16}$$

It is useful to introduce $g(r)=\frac{4}{(1+r^2)^2}$ so that the metric becomes

$$g_{ij} = g(r)\delta_{ij}. \tag{3.17}$$

In the UV the impurity extend into the bulk of AdS_3, i.e. they are of the type discussed in section 3.1.1, so that it is natural to choose (t,z) as the brane's worldvolume coordinates. On the S^3 factor the branes are pointlike, as discussed in section 3.1.2 or also in section A.2.2. Without loss of generality, their locus on the S^3 can be chosen to be the north pole, $\vec{y}=0$ in stereographic coordinates. Together, the branes are of D1 type in the full geometry $AdS_3\times S^3\times T^4$.

With the setup fixed, we study a deformation of the system in which the S^3 embedding coordinate matrix $\vec{y}$ of these D1-branes becomes non-commutative, indicated in boldface,

$$y^i \to \mathbf{y}^i = \lambda f(z)\mathbf{\Sigma}_i\,, \tag{3.18}$$

We allowed for a non-trivial z-profile $f(z)$. The Hermitian matrices $\mathbf{\Sigma}_i$ furnish a representation of $\mathfrak{su}(2)$,

$$[\mathbf{\Sigma}_i,\mathbf{\Sigma}_j] = i\epsilon_{ijk}\mathbf{\Sigma}_k\,. \tag{3.19}$$

By assuming that the fundamental of $\hat{\mathfrak{u}}(k)$ is irreducible under $\mathfrak{su}(2)$, it can be identified with the spin $\frac{k-1}{2}$ representation. Consider the radial coordinate in polar coordinates, $\mathbf{r}^2=\vec{\mathbf{y}}^2 = C_2(\Sigma)(\lambda f)^2\mathbf{1}$, where $C_2(\Sigma)=\frac{k^2-1}{4}$ is the quadratic Casimir of $\mathfrak{su}(2)$ in the representation

defined by $\vec{\mathbf{\Sigma}}$. It is evident from this that r is still an abelian object, $r = \sqrt{C_2}\lambda f$. We further assume that the brane has a fixed location in the spatial coordinate x inside AdS_3 and the M_4 directions[7].

The non-abelian DBI Lagrangian takes the form

$$I_{\text{DBI}} = -T_{\text{D1}}\text{Tr}\left(e^{-\Phi}\sqrt{-\det(E_{ab} + E_{ai}(Q^{-1} - \delta)^{ij}E_{jb} + \lambda F_{ab})\det(Q^i{}_j)}\right), \tag{3.20}$$

where T_{D1} is the tension of a D1-brane and

$$E_{\mu\nu} = g_{\mu\nu} + B_{\mu\nu} \tag{3.21}$$

$$Q^i{}_j = \delta^i{}_j - i\lambda[\mathbf{y}^i, \mathbf{y}^k]E_{kj}\,. \tag{3.22}$$

In this expression, $\xi^a = (t, z)$ denote the worldvolume variables, while y^i denote the transverse variables. Recall from section 3.1.1 that $F_{ab} = 0$, $\psi = 0$, $B_{\text{AdS}_3} = 0$ for a pure D1-string impurity.

The relevant components of $E_{\mu\nu}$ can then be approached,

$$\begin{aligned} E_{ij} &= L^2\left(g\,\delta^i{}_j + \frac{b(\theta(r))}{r^2}\epsilon_{ijk}\mathbf{\Sigma}^k\right), \\ E_{ab} &= g_{ab}, \\ E_{ia} &= 0 = E_{ai}, \end{aligned} \tag{3.23}$$

and also[8]

$$Q^i{}_j = \left(1 - \frac{2L^2 b}{\lambda\sqrt{C_2}}\right)\delta^i{}_j\mathbf{1} + \frac{2L^2 b}{\lambda(C_2)^{3/2}}\mathbf{\Sigma}^j\mathbf{\Sigma}^i + \frac{2L^2}{\lambda C_2}r^2\,g\,\epsilon_{ijk}\mathbf{\Sigma}^k \tag{3.24}$$

Then

$$-\det(E_{ab} + E_{ai}(Q^{-1} - \delta)^{ij}E_{jb}) = \frac{L^2}{z^2}\left(\frac{L^2}{z^2} + \frac{(\partial_z r)^2}{C_2}\mathbf{\Sigma}^i\left(Q^{-1}\right)_{ij}\mathbf{\Sigma}^j\right) \tag{3.25}$$

where $Q^{ij}(Q^{-1})_{jk} = \delta^i{}_k$ with $Q^{ij} = E^{ij} - i\lambda[\mathbf{\Sigma}^i, \mathbf{\Sigma}^j]$ and $E^{ij}E_{jk} = \delta^i{}_k$.

The dimension of the perturbing operator θ lurks inside the potential generated by the action (3.20). Actually, we only require the mass term, $\mathcal{O}(\theta^2)$. We anticipate that the mass term vanishes, indicating that the perturbation is classically marginal. Hence, we carry out the computation out to $\mathcal{O}(\theta^3)$. They contain the information on whether the operator is marginally relevant or marginally irrelevant.

Inspection of (3.25) together with $r = \tan\theta/2$ makes clear no pure powers of θ appear in this determinant. Instead, only derivatives of θ in z pop up. Hence, it suffices to expand its contributions to leading order, $\left(Q^{-1}\right)_{ij} = 4L^2\delta^i{}_k + \mathcal{O}(\theta)$ and $r = \theta/2 + \mathcal{O}(\theta^3)$. This yields

$$-\det(E_{ab} + E_{ai}(Q^{-1} - \delta)^{ij}E_{jb}) = \frac{L^2}{z^2}\left(\frac{L^2}{z^2} + L^2(\partial_z\theta)^2\right) + \ldots \tag{3.26}$$

No powers of θ are found in this expression. The important terms must therefore reside in the remaining determinant in (3.20). Indeed, it presents us with the correct orders when expanding (3.24) and recalling $r^2\,g = \sin^2\theta$,

$$Q^i{}_j = \delta^i{}_j + \theta^2\frac{2L^2}{\lambda C_2}\epsilon_{ijk}\mathbf{\Sigma}^k + \theta^3\frac{4}{3(C_2)^{3/2}\lambda}\left(\mathbf{\Sigma}^j\mathbf{\Sigma}^i - C_2\delta^i{}_j\right), \tag{3.27}$$

[7] In Janus coordinates on AdS_3 the coordinate ψ indicating the AdS_2 slice is also chosen to be an abelian constant in our ansatz.

[8] We refrain from matching the indices on both sides of (3.24), because raising and lowering involves E^{ij}.

providing

$$\sqrt{Q^i{}_j} = \left(1 - \theta^3 \frac{4}{3(C_2)^{1/2}}\right)\mathbf{1} + \mathcal{O}(\theta^4). \tag{3.28}$$

Piecing everything together, we find for the non-abelian DBI action

$$e^{\Phi} I_{\text{DBI}} = \frac{L^2}{z^2} + \frac{L^2}{2}(\partial_z\theta)^2 - \frac{L^2}{z^2}\frac{4L^2}{3\lambda\sqrt{C_2}}\,\theta^3 + \dots\,, \tag{3.29}$$

As anticipated, this carries no mass term. Hence, the operator is classically marginal. Furthermore, the cubic order is negative, indicating that the UV fixed point is repulsive. Therefore, the operator is a marginally relevant perturbation, as is the case in the actual Kondo model! In conclusion, we have found that a flow with Kondo-like properties is indeed tripped starting with a D1-brane impurity embedded into the $\text{AdS}_3 \times \text{S}^3 \times T^4$ geometry.

3.3 Supersymmetric $\text{AdS}_2 \times S^2$ Branes as RG Fixed Point

Now that we know that the flow is tripped in the UV, we would like to know if the configuration stops renormalizing at some point. That is, we investigate the r.h.s. of (3.2). Thinking again of the brane condensation process in section 2.3 as blueprint, we expect to find that the pointlike configuration becomes large against the string scale and puffs up into a D3-brane into which the D1-branes have dissolved. If appropriate, the RG flow should stop at some value of polar angle on the S^3 determined by the number of D1-branes in the UV configuration. The discussion in this section follows closely that of [2].

Coordinates are chosen as before on the constituents of $\text{AdS}_3 \times \text{S}^3$,

$$ds^2 = L^2\left[\frac{dz^2 - dt^2 + dx^2}{z^2} + d\theta^2 + \sin^2\theta\left(d\phi^2 + \sin^2\phi\, d\chi^2\right)\right]. \tag{3.30}$$

Supersymmetry forces the radii of AdS_3 and S^3 coincide. For the worldvolume of the D3-brane we choose coordinates

$$\xi^a = (z,\, t;\, \phi,\, \chi), \qquad \text{static gauge}, \tag{3.31}$$

which leaves us with two fluctuating fields, $x = x(\xi)$ and $\theta = \theta(\xi)$. Kondo-like physics should respect $SU(2)$ invariance. This is easily achieved by demanding that all quantities be independent of the two-sphere coordinates $(\phi,\, \chi)$. For our purposes, it suffices to consider static situations, leaving us with $x = x(z)$ and $\theta = \theta(z)$. Because the holographic direction z is an energy scale, a z-dependence determines how all fields renormalize along the RG flow, in particular the polar angle $\theta(z)$. It characterizes how far the S^2 part of the D3-brane slides down on the S^3. If it stops at some fixed value, the flow has a non-trivial IR fixed point. Indeed, this will be the case and the polar angle will saturate at the obvious suspect θ_p, see (3.12).

As usual, the spacetime metric g needs to be pulled back onto the worldvolume,

$$\hat{g} = L^2(z^{-2} + x'^2 + \theta'^2)dz^2 - \frac{L^2}{z^2}dt^2 + \sin^2\theta\left(d\phi^2 + \sin^2\phi\, d\chi^2\right). \tag{3.32}$$

When considering the $U(1)$ field strength, $F = F_{ab}\, d\xi^a \wedge d\xi^b$, it pays off to extract guidelines from the original Kondo effect. First of all, $SU(2)$ invariance is required, and demanding it forbids crossterms between the AdS_2 and S^2 parts,

$$F = F_{zt}\, dz \wedge dt + F_{\phi\chi}\, d\phi \wedge d\chi. \tag{3.33}$$

Of course, this also secures an $SO(2,1)$ symmetry appropriate for an interface in two-dimensional CFT. Furthermore, we employ the results of [60, 61], which are collected in section 3.1, as an ansatz[9]

$$\begin{aligned} x'(z) &= 0, \\ F_{zt} = 0, \qquad F_{\phi\chi} &= -\frac{p}{2}\sin\phi. \end{aligned} \tag{3.34}$$

With this ansatz, the gauge invariant field strength is pieced together from the individual pieces (3.7) and (3.13)[10],

$$\begin{aligned} \mathcal{F} =& \mathcal{F}_{\text{AdS}} + \mathcal{F}_{\text{S}} = L^2\big(b(\theta) - \theta_p\big)\sin\phi, \\ b(\theta) :=& \ \theta - \sin\theta\cos\theta, \end{aligned} \tag{3.35}$$

with θ_p as before, (3.12). For interfaces with fundamental string charge, $q \neq 0$, the gauge invariant field strength contains also a contribution from AdS_3, c.f. [1]. At last, all ingredients for the DBI action of this system are assembled,

$$\begin{aligned} S_{DBI} &= \int dt\, \mathsf{L} \\ &= -T_3 \int dz\, dt\, d\phi\, d\chi\, \sqrt{-\det(\hat{g} + \mathcal{F})} \\ &= -4\pi L^2\, T_3 \int dz\, dt\, \frac{L^2}{z^2}\sqrt{NP}, \end{aligned} \tag{3.36}$$

where L is the Lagrange function of the system and

$$N = 1 + (z\theta')^2, \tag{3.37}$$

$$P = \sin^4\theta + (b(\theta) - \theta_p)^2. \tag{3.38}$$

The prefactor $4\pi L^2$ stems from integrating the two-sphere coordinates (ϕ, χ), which is straightforwardly done, since nothing depends on them. As usual, the next step is to solve the equations of motion,

$$0 = \theta'' - z\theta'^3 - 2\Lambda_p(\theta)\sin^2\theta\frac{1 + (z\theta')^2}{z^2(\sin^4\theta + (b(\theta) - \theta_p)^2)}. \tag{3.39}$$

Even though it is just an ordinary differential equation, it is quite difficult to solve.

In order to make progress, we turn to an elegant alternative approach employed in higher dimensions in [62] and applied to this case in [2]. It is based on a careful analysis of the system's energy, in particular its minima, which are constant in RG time z. Since the radial coordinate in AdS has an interpretation as energy scale, these configurations are those for which renormalization stopped.

The Hamilton function H of the system, given by the Legendre transformation of the Lagrange function L in (3.36),

$$\mathsf{H} = \dot{\theta}\frac{\partial\mathsf{L}}{\partial\dot{\theta}} + \dot{A}_z\frac{\partial\mathsf{L}}{\partial\dot{A}_z} + \dot{A}_t\frac{\partial\mathsf{L}}{\partial\dot{A}_t} - \mathsf{L} = 4\pi L^2\, T_3 \int dz\frac{L^2}{z^2}\sqrt{NP}. \tag{3.40}$$

[9] We stress that this review only discusses the simplest interface, i.e. with fundamental string charge $q = 0$. The most general class, with $q \neq 0$ was first discussed in [1]. In that case, the correct ansatz for the spatial coordinate is $x' =$ constant. An extensive review on flows of these interfaces is found in [2].

[10] In the first line of (3.36) L means Lagrange function, while in the last line of the same equation it means the AdS radius.

Because we are looking at a static setup and we have gauged $A_z = 0$, the first three momentum terms vanish, giving way for the second equality.

Configuration in which the polar angle $\theta(z)$ has stopped renormalizing have $\theta'(z) = 0$ and they minimize the energy locally,

$$0 \stackrel{!}{=} \frac{\partial \mathsf{H}}{\partial \theta}\bigg|_{\theta'=0} = 4\pi L^2\, T_3 \int dz \frac{L^2}{z^2}\sqrt{\frac{N}{P}}\, 2(\theta - \theta_p)\sin^2\theta. \tag{3.41}$$

It is useful to contemplate the polar angle in relation to (3.12). Hence, in analogy to [62] it is useful to define[11]

$$\Lambda_p(\theta) := \theta - \theta_p. \tag{3.42}$$

Evidently, three local energy minima arise from (3.41),

$$\Lambda_p(\theta)\, \sin^2\theta = 0 \qquad \Rightarrow \qquad \theta = 0,\, \pi,\, \theta_p. \tag{3.43}$$

The brane has no extension on three-sphere for $\theta = 0, \pi$, while the configuration corresponding to θ_p describes a $D3 = \mathrm{AdS}_2 \times \mathrm{S}^2$. In fact, the θ_p is the global minimum. Indeed, evaluation of the energy (3.40) on these configurations with $\theta' = 0$ yields

$$\mathsf{H}(\theta = 0) = \mathsf{H}(\theta = \pi) = 4\pi L^2\, T_3 |\theta_p| \int dz \frac{L^2}{z^2}, \tag{3.44}$$

$$\mathsf{H}(\theta = \theta_p) = 4\pi L^2\, T_3 |\sin\theta_p| \int dz \frac{L^2}{z^2}. \tag{3.45}$$

A comparison of these two energy values confirms that the non-trivial polar angle θ_p is the global energy minimum,

$$\frac{\mathsf{H}(\theta_p)}{\mathsf{H}(0)} = \left|\frac{\sin\theta_p}{\theta_p}\right| \leq 1. \tag{3.46}$$

This is the first important result: A D3= $\mathrm{AdS}_2 \times \mathrm{S}^2$ appears as local and global energy minimum. It is therefore the most natural candidate for the IR fixed point. In order to truly establish it as the IR fixed point, we need to confirm that renormalization indeed stops at θ_p. To this end, we have to find solutions to the equations of motion.

Now we return to the general situation, where the polar angle θ depends on the radial coordinate z and recast the Hamilton function (3.40) in the form

$$H = 4\pi L^4 T_3 \int dz\, \sqrt{\mathcal{Y}^2 + \mathcal{Z}^2}. \tag{3.47}$$

This employs

$$z^2\mathcal{Y} = \Lambda_p \sin\theta + z\theta'(\sin\theta - \Lambda_p\cos\theta), \tag{3.48}$$

$$z^2\mathcal{Z} = z\theta'\Lambda_p\sin\theta - (\sin\theta - \Lambda_p\cos\theta) = z^2\frac{d}{dz}\frac{\sin\theta - \Lambda_p\cos\theta}{z}. \tag{3.49}$$

This form of the Hamilton function grants easy access to the lower bound

$$H \geq 4\pi L^4 T_3 \int dz |\mathcal{Z}|. \tag{3.50}$$

Here comes the magic of this approach. Because $\mathcal{Z}$ is a total derivative, the bound is easily integrated! It is found to depend only on the boundary values of $\theta(z)$. Any configuration

[11] Readers interested in comparing with [62] are advised that our p corresponds to their n.

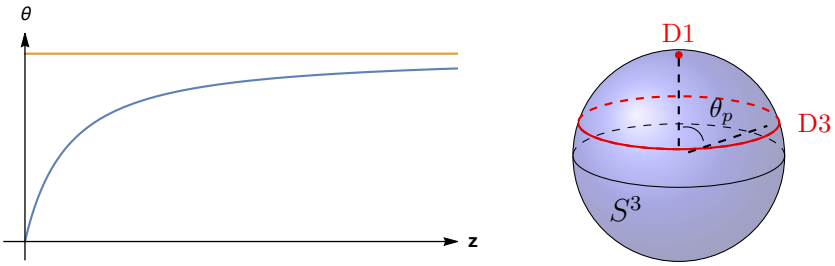

Figure 6: Left: Plot of the RG dependence of the polar angle θ given by (3.52). It saturates at the yellow line, which demarcates $\theta_p = \pi p/N_5$. Right: In the UV we have a stack of F1 strings, which condense in the IR into a single D3-brane at θ_p. This figure appeared before in [2]. (For interpretation of the references to color in this figure legend, the reader is referred to the web version of this article [https://jhap.du.ac.ir/].)

$\theta(z)$ saturating the bound automatically solves the equations of motion. From (3.47) it is evident that this happens when $\mathcal{Y} = 0$. This provides the first order differential equation,

$$z\theta' = -\frac{\Lambda_p \sin\theta}{\sin\theta - \Lambda_p \cos\theta}. \tag{3.51}$$

It is evident that this equation is much more accessible than the equation of motion (3.39), justifying our approach. Integrating (3.51) gives

$$z(\theta) = z_0 \frac{\sin\theta}{\theta - \theta_p}. \tag{3.52}$$

This equation can be inverted to give an implicit dependence $\theta(z)$. It is not necessary to do so, however, if we are just interested in pinpointing the fixed points. It suffices to look for values of θ for which the RG time z diverges. It is at these points that renormalization stops. Evidently, this happens for $\theta = \theta_p$. Note that neither $\theta = 0$ nor $\theta = \pi$ fulfill this requirement, ruling them out once and for all from being the sought after energy minimum. A plot of (3.52) confirms that as z increases, moving further into the bulk of AdS_3, the polar angle saturates at $\theta = \theta_p$, see figure 6.

The flow described here preserves a number of supersymmetries. Indeed, the first order differential equation (3.51) generates solutions to the equations of motion (3.39). This characteristic is a hallmark of BPS equations, and thus the flow preserves half of the supersymmetries of the full system. How many are those? The near-horizon region of the F1/NS5 system has sixteen superconformal symmetries. The presence of the defect breaks these down to eight superconformal symmetries. The flow, being BPS, then preserves only four supercharges. Since the perturbation is marginally relevant, conformality is lost along the flow and recovered only at the IR fixed point, where eight superconformal charges arise again.

Certainly, there can exist other flows, which break all supersymmetry. Such are solutions to the equations of motion (3.39), but not (3.51). Altogether, we have thus found a very special class of flows, namely those which preserve the maximal number of supercharges.

The discussion provided in this section appeared in [2]. When considering the larger class of flows, which have a (p, q)-string in the UV rather than just D1-branes, the route taken here is not well suited any longer. The reason is that the analogs of $\mathcal{Y}$ and $\mathcal{Z}$ are difficult to find. Therefore, in [1], a different framework was chosen for interfaces with additional F1

charge q. Changing to the S-dual frame, the D1/D5 background, the flows are found through use of *κ-symmetry*. Reparametrizations in general relativity are bosonic symmetries, and κ-symmetry realizes their fermionic superpartners.

In conclusion, we have indeed confirmed that Kondo-like flow exist in the F1/NS5 system, in the sense that they are described by a brane condensation, as in section 2.3. The construction here was in the probe brane limit. In the next section, we take a thorough look at the fixed points, including the full backreaction of the impurity on the ambient F1/NS5 system.

4 Supergravity duals of the fixed points

So far, we uncovered the existence Kondo-like flows in holography. In order to achieve this, we treated the interface branes as probes pretending that they have no influence on the F1/NS5 background, in which they move. This description is in fact only accurate, whenever the interface charge is much smaller than that of the background. In general, we are interested in interfaces, whose charge is of the order of the background's. This means that these impurities are heavy objects, which curve their environment. Hence, backreaction becomes important.

Of course, it is desirable to have a fully backreacted description of the flows. After all, the AdS/CFT conjecture is, in its weak form, a duality of a field theory with supergravity, not just the probe limit. In general, gravitational backreaction is important when matching gravity results to those in the CFT. Examples are correlation functions, in particular one point functions, which measure the expectation values of fields in the presence of an interface, but also reflection and transmission coefficients across the defect [63].

Having a fully backreacted supergravity solution dual to the RG flow in the field theory, is equivalent to having a geometry which smoothly deforms from the UV gravity dual to the IR gravity dual. This is a very ambitious task. Its first hurdle was taken in [1,2] by deriving the fully backreacted gravity duals of the fixed points of the RG flow.

The construction is based on the general class of solutions to type IIB supergravity with $\mathrm{AdS}_3 \times S^3 \times T_4$ asymptotic presented in [49]. These geometries are foliated by $\mathrm{AdS}_2 \times S^2$ submanifolds and preserve 8 super(conformal) symmetries, rendering them dual to superconformal defects in 2d CFT. The T_4 factor has no internal fluxes in these solutions and has constant moduli, apart from its size.

The solutions for the impurities in the F1/NS5 system discussed in the following appeared first in [2]. Their S-duals, i.e. impurities in the D1/D5 frame, were derived in [1]. Both of these references contain the most general class of interfaces, meaning that they harbor D1 and F1 charge. In this review, we are mainly concerned with the simplest case, so that only the case of D1 impurities inside the F1/NS5 system are described here. Moreover, the detailed derivation of these solutions would take us too far afield with technicalities. Therefore, the solutions are only presented rather than derived in this review. Interested readers are referred to [1,2] for detailed derivations.

We begin in section 4.1 by collecting the required details for the presentation of the impurity solutions. While these are general, applying to any geometry with $\mathrm{AdS}_3 \times S^3 \times T^4$ asymptotics and eight superconformal charges, in going on we narrow down to the case of the F1/NS5 system. As a warm-up, we present the pure F1/NS5 geometry in section 4.2. The D1 interface is installed in this geometry in section 4.3 and, thereafter, the D3 interface with dissolved D1 charge is presented in section 4.4. Both solutions exist independently of each other a priori. We connect them via our Kondo-like flows in section 4.5, finding agreement with the results of the previous chapter. Finally, we describe the limit of critical

screening in section 4.6. Throughout our description, Page charges play a central role. Their details are collected in appendix B.

4.1 Supergravity Duals of Conformal Interfaces in CFT_2

In order to write down type IIB supergravity solutions incorporating Kondo-like RG flows, consider the general class of half-BPS solutions of [49]. The solutions considered here possess two asymptotic regions with $AdS_3 \times S^3 \times M_4$ geometry. A specific class solutions with multiple $AdS_3 \times S^3 \times M_4$ asymptotic regions was provided in [55, 64].

The ten-dimensional geometries of interest have a line element of the form

$$ds_{10}^2 = f_1^2 ds_{AdS_2}^2 + f_2^2 ds_{S^2}^2 + f_3^2 ds_{T_4}^2 + \rho^2\, dz\, d\bar{z}. \tag{4.1}$$

Here, $ds_{AdS_2}^2$, $ds_{S^2}^2$, $ds_{T_4}^2$ are unit radius metrics for the subscripted geometries. The last piece, $\rho^2\, dz\, d\bar{z}$, is the metric of a Riemann surface Σ with boundary. It stands out, because the remaining line elements depend on Σ, i.e. $f_i = f_i(z, \bar{z})$ with $i = 1, 2, 3$. Positive definiteness of the metric secures that the metric factors f_i and ρ be real and positive-definite functions on Σ. They are

$$f_1^2 = \frac{e^{\phi}}{2f_3^2}\frac{|v|}{u}(a\,u + \tilde{b}^2), \tag{4.2a}$$

$$f_2^2 = \frac{e^{\phi}}{2f_3^2}\frac{|v|}{u}(a\,u - b^2), \tag{4.2b}$$

$$f_3^4 = e^{-\phi}\frac{u}{a}, \tag{4.2c}$$

$$\rho^4 = 4e^{-\phi}u\left|\frac{\partial_z v}{B}\right|^4 \frac{a}{v^2} \tag{4.2d}$$

where four harmonic functions[12]

$$\begin{aligned} a &= A + \bar{A}, \qquad & b &= B + \bar{B}, \\ u &= U + \bar{U}, \qquad & v &= V + \bar{V} \end{aligned} \tag{4.3}$$

and their duals

$$\begin{aligned} \tilde{a} &= -i(A - \bar{A}), \qquad & \tilde{b} &= -i(B - \bar{B}), \\ \tilde{u} &= -i(U - \bar{U}), \qquad & \tilde{v} &= -i(V - \bar{V}). \end{aligned} \tag{4.4}$$

have been employed. The harmonic functions decompose into holomorphic functions $A(z)$, $B(z)$, $U(z)$, $V(z)$ and their anti-holomorphic counterparts $\bar{A}(\bar{z})$, $\bar{B}(\bar{z})$, $\bar{U}(\bar{z})$, $\bar{V}(\bar{z})$. Any solution to the setup of [49] is specified by these eight functions. Positivity of the metric factors imposes $a \geq 0$, $u \geq 0$ and $au - b^2 \geq 0$.

The expressions for the dilaton ϕ, axion χ and Ramond-Ramond four form are

$$e^{-2\phi} = \frac{1}{4u^2}(a\,u - b^2)(a\,u + \tilde{b}^2), \tag{4.5a}$$

$$\chi = \frac{1}{2u}(b\,\tilde{b} - \tilde{a}\,u), \tag{4.5b}$$

$$C_K = \frac{1}{2a}(b\,\tilde{b} - a\,\tilde{u}). \tag{4.5c}$$

[12] Reference [49] uses supergravity conventions in which the RR four-form is a factor 4 to small for our purposes. We rescale to string theory conventions, by setting $\mathrm{Hol}(\hat{h}) = U/4$ and shift $B \to B/2$. Since we use capital letters for meromorphic functions we write $V = \mathrm{Hol}(H)$.

Here, C_K is the component of $C_{(4)} = C_K\,\omega_{T^4} + C_{\mathrm{AdS}_2,S^2}\,\omega_{\mathrm{AdS}_2}\wedge\omega_{S^2}$ along the T^4 directions. The remaining component along the combined directions of S^2 and AdS_2, C_{AdS_2,S^2} is related to C_K via self-duality of $F_{(5)}$. In this review, all ω denote unit volume forms on the indicated geometries.

Singularities in f_1 designate asymptotic $\mathrm{AdS}_3\times S^3\times T^4$ regions, which translates into poles of V. The interfaces described in this review glue two CFTs and thus the geometries here have two asymptotic regions. Parameterizing Σ by a complex coordinate z, we anticipate that the asymptotic regions lie at $z=0$ and $z\to\infty$.

Each asymptotic region is best described in terms of their Page charges Q_{brane}, which are collected in appendix B. Mostly, we employ rescaled Page charges,

$$q_{D5}\equiv\frac{Q_{D5}}{8\pi^2},\qquad q_{NS5}\equiv\frac{Q_{F5}}{8\pi^2},\qquad q_{D1}\equiv\frac{Q_{D1}}{8\pi^2},\qquad q_{F1}\equiv\frac{Q_{F1}}{8\pi^2}\tag{4.6}$$

The central charge of the asymptotic region is given by the Brown-Henneaux formula and can be expressed in terms of the Page charges,

$$\mathsf{c}=\frac{3\mathsf{L}}{2G_N^{(3)}}=\frac{96\pi^3}{\kappa_{10}^2}\Big(q_{D5}\,q_{D1}+q_{NS5}\,q_{F1}\Big).\tag{4.7}$$

where the ten-dimensional gravitational constant and the ten-dimensional Newton constant are

$$\kappa_{10}^2=8\pi G_N^{(10)},\tag{4.8}$$

$$G_N^{(10)}=G_N^{(3)}\,\mathrm{Vol}(S^3_{\mathsf{L}})\,\mathrm{Vol}(T^4_{f_3})=G_N^{(3)}\,2\pi^2\mathsf{L}^3\,f_3^4,\tag{4.9}$$

where the subscripts in the volumes denote the respective radii[13] and L is the ten-dimensional AdS radius. A general expression for L is found in [2,64]. In this review, we content ourselves with providing the particular expression for L for the asymptotic regions in each individual geometry of interest. It is also convenient to define the six-dimensional AdS radius,d $z\to\infty$.

$$\mathsf{R}^4=\mathsf{L}f_3=4\Big(q_{D5}\,q_{D1}+q_{NS5}\,q_{F1}\Big)=\frac{4G_N^{(10)}}{\mathrm{Vol}(S^3)}\frac{\mathsf{c}}{6}\tag{4.10}$$

The charges differ depending on the asymptotic region. In order to distinguish them, we place superscripts on them, for instance the value of the $F5$ charge at the asymptotic regions $z=0$ and $z\to\infty$ are denoted $q_{NS5}^{(0)}$ and $q_{NS5}^{(\infty)}$, respectively. Similarly, the fields (4.5) are assigned a label when evaluated at the asymptotic regions, e.g. the dilaton at $z=0$ is $\phi(0)$ and at $z\to\infty$ it is $\phi(\infty)$.

In the following sections we provide the F1/NS5 geometry using this setup and augment it subsequently by a D1 interface and a D3 interface.

4.2 The F1/NS5 Geometry

To showcase the formalism laid out in the previous section, we provide its description of the F1/NS5 geometry. Since it carries no interface, we refer to it as the vacuum. A detailed derivation of this is found in [2].

[13] Whenever we omit the radius in Volume expression it implies unit radius, i.e. $\mathrm{Vol}(S^3)=2\pi^2$

The vacuum meromorphic functions are

$$V(z) = i\nu\big(z^{-1} - z\big), \qquad v = 2\nu\frac{\Im(z)}{|z|}\big(|z|^{-1} + |z|\big), \tag{4.11a}$$

$$A(z) = i\alpha\big(z^{-1} - z\big), \qquad a = 2\alpha\frac{\Im(z)}{|z|}\big(|z|^{-1} + |z|\big), \tag{4.11b}$$

$$B(z) = -i\beta\big(z^{-1} + z\big), \qquad b = -2\beta\frac{\Im(z)}{|z|}\big(|z|^{-1} - |z|\big), \tag{4.11c}$$

$$U_0(z) = i\eta\big(z^{-1} - z\big), \qquad u_0 = 2\eta\frac{\Im(z)}{|z|}\big(|z|^{-1} + |z|\big). \tag{4.11d}$$

where β is constrained by $\beta^2 = \alpha\eta$. Therefore, the four meromorphics depend only on three parameters. We have place a subscript on the function $U \to U_0$, as it is modified below by the interfaces. All other function retain the same shape.

In order to access the physical significance of the parameters ν, α, η they need to be expressed in terms the existing charges and the dilaton q_{NS5}, q_{F1}, ϕ[14],

$$q^{(0)}_{NS5} = \frac{\nu}{\sqrt{\alpha\,\eta}} = -q^{(\infty)}_{NS5}, \tag{4.12a}$$

$$q^{(0)}_{F1} = 4\nu\sqrt{\alpha\,\eta} = -q^{(\infty)}_{F1}, \tag{4.12b}$$

$$e^{-2\phi(0)} = 4\alpha^2 = e^{-2\phi(\infty)}. \tag{4.12c}$$

Note sign difference of the charges between asymptotic regions, which secures charge conservation in the full geometry. These equations can be inverted to

$$\nu = \frac{1}{2}\sqrt{q^{(0)}_{NS5}\,q^{(0)}_{F1}}, \qquad \alpha = \frac{1}{2}e^{-\phi(0)}, \qquad \eta = \frac{1}{2}\frac{q^{(0)}_{F1}}{q^{(0)}_{NS5}}e^{\phi(0)}. \tag{4.13}$$

The constraint parameter β is given by $\beta^2 = \alpha\eta = \frac{q^{(0)}_{F1}}{4q^{(0)}_{NS5}}$. This dependence may have been just as well in terms of the charges and dilaton at $z \to \infty$. Given the functions (4.11) the combined metric factors (4.2) give rise to $\mathrm{AdS}_3 \times S^3 \times T^4$ for any point on Σ, i.e. not just asymptotically so. This feature changes once interfaces are installed in the geometry. In coordinates $z = \exp(\psi + i\theta)$ and employing (4.13) the metric becomes

$$ds^2_{10} = \mathsf{L}^2\left(d\psi^2 + \cosh^2\psi\, ds^2_{\mathrm{AdS}_2} + d\theta^2 + \sin^2\theta ds^2_{S^2}\right) + \sqrt{\frac{q^{(0)}_{F1}}{q^{(0)}_{NS5}}e^{\phi(0)}}ds^2_{T^4}, \tag{4.14}$$

with ten-dimensional AdS radius $\mathsf{L}^2 = 2q^{(0)}_{NS5}e^{-\phi(0)/2} = 2|q^{(\infty)}_{NS5}|e^{-\phi(\infty)/2}$.

Comparison of (4.14) to the F1/NS5 Einstein frame solution in the literature, the Page charges can be related to the integer valued charges N_1, N_5,

$$Q_{NS5} = 8\pi^2 q_{NS5} = (2\pi)^2\alpha' N_5, \qquad Q_{F1} = 8\pi^2 q_{F1} = (2\pi)^6\alpha'^3 N_1, \tag{4.15}$$

and similarly for Q_{D5} and Q_{D1}. Plugged into the central charge (4.7) together with $4\pi\kappa^2_{10} = (2\pi)^8\alpha'^4$ we obtain the well known result $\mathsf{c} = 6N_1N_5$.

In the following interfaces will be inserted into this vacuum solution by modifying the function (4.11d). This augments the expressions in (4.13) by interface charges in such a way that they reduce to the vacuum solution when shrinking the interface charge to zero. In this line of thought, the vacuum may be interpreted as the trivial interface.

[14] This geometry does not carry D1 or D5 charge

4.3 D1 Interface

Now that the vacuum solution is at our disposal, we modify it such that it harbors a D1 interface. Readers interested in seeing the more general class of $D1/F1$ interfaces within the F1/NS5 geometry are directed to [2]. The S-udal of these solutions, i.e. F1/D1 interfaces within the D1/D5 geometry, appeared in [1]. As before, we only present the geometry, not its derivation, which is found in aforementioned references.

A D1 interface is induced by adding a pole at $\xi \in \partial\Sigma = \mathbb{R}$ to the function (4.11d)

$$U(z) = U_0 + \delta U^{D1}, \qquad \delta U^{D1} = ic\,\frac{\xi}{z-\xi}, \qquad \delta u^{D1} = \frac{2c\,\xi\,\Im(z)}{|z-\xi|^2}. \tag{4.16}$$

while retaining the shape of the remaining functions in (4.13) fixed. W.l.o.g., we choose $\xi > 0$. Negative ξ simply means that the brane lies on the upper boundary of the strip Σ, which corresponds to $\theta = \pi$, see figure 7. The brane inside $\mathrm{AdS}_3 \times \mathrm{S}^3$ is depicted in figure 8. We note that this one-brane interfaces is smeared over the T_4 directions. The value of ξ determines the F1 charge of the brane. No F1 charge is present, when $\xi = 1$, and in the following, we restrict to this case. In strip coordinates $w = \log z = \psi + i\theta$ this means that $w_\xi = \log\xi = 0$.

The constant $c \geq 0$ is tied to the D1 charge of the interface as follows,

$$q^{\mathcal{D}}_{D1} \equiv -q^{(0)}_{D1} - q^{(\infty)}_{D1} = -c\,q^{(0)}_{NS5}, \tag{4.17}$$

Because the brane carries no F1 charge, by charge conservation the asymptotic regions have still the same central charge as in the vacuum solution, $\mathsf{c} = 6N_1N_5$. However, the asymptotic values of the RR four-form are affected

$$C_K(0) = -c = \frac{q^{\mathcal{D}}_{D1}}{q^{(0)}_{NS5}}, \qquad C_K(\infty) = 0. \tag{4.18}$$

This is why the brane cannot be a defect, but is rather an interface. In contrast, the dilaton remains the same at both asymptotic regions[15],

$$e^{-2\phi(\infty)} = -e^{-2\phi(0)}. \tag{4.19}$$

The axion vanishes at both asymptotic regions.

Since the F1 charges coincide at both asymptotic regions their superscripts can be dropped, $q_{F1} \equiv q^{(0)}_{F1} = -q^{(\infty)}_{F1} = \overline{q_{F1}}$. Similarly for the F5 charge $q_{NS5} \equiv q^{(0)}_{NS5} = -q^{(\infty)}_{NS5} = \overline{q_{NS5}}$. Similar to the vacuum solution, the D1 interface is determined by a set of holomorphic functions (4.11), where (4.11d) is modified by (4.16). The parameters are

$$\nu = \frac{1}{2}\sqrt{\frac{q_{NS5}\,q_{F1}}{\kappa_0}}, \qquad \alpha = \frac{1}{2\sqrt{\kappa_0}}e^{-\phi(0)}, \qquad \eta = \frac{1}{2\sqrt{\kappa_0}}\frac{q_{NS5}}{q_{F1}}e^{\phi(0)}, \qquad c = \frac{|q^{\mathcal{D}}_{D1}|}{q_{NS5}}, \tag{4.20}$$

where,

$$\kappa_0 \equiv \kappa(q^{\mathcal{D}}_{D1},\,0) = \frac{T_{(4q^{(0)}_{F1},\,q^{\mathcal{D}}_{D1})} + T_{(0,\,q^{\mathcal{D}}_{D1})}}{T_{(4q^{(0)}_{F1},\,q^{\mathcal{D}}_{D1})} - T_{(0,\,q^{\mathcal{D}}_{D1})}}. \tag{4.21}$$

This is controlled by the string tension of a (p,q)-string,

$$T_{(p,q)} = \sqrt{p^2T^2_{D1} + q^2T^2_{F1}} \tag{4.22}$$

The parameter β is determined, as in the vacuum solution, by $\beta^2 = \alpha\eta$.

The interface vanishes in the limit $c \to 0$, i.e. $q^{\mathcal{D}}_{D1} \propto c \to 0$ leading to $\kappa_0 \to 1$ and therefore the triple (α,η,ν) reduces to those of the vacuum (4.13).

[15] The dilaton does differ at the asymptotic regions, when the interface carries F1 charge.

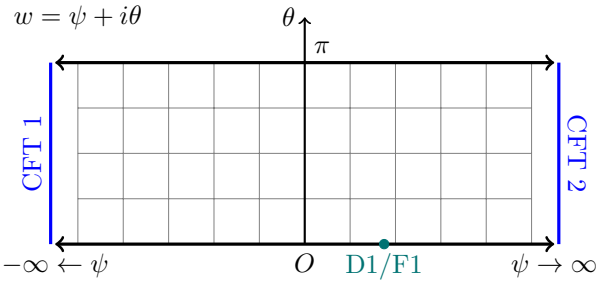

Figure 7: Using strip coordinates $w = \log z = \psi + i\theta$ on Σ, the two asymptotic regions, depicted by blue bars, lie at $\psi \to \pm\infty$. Each harbors a CFT and they differ due to the presence of the D1/F1 interface located at $\xi \in \partial\Sigma$ depicted as red dot. The lower boundary, $\theta = 0$, corresponds to the north pole of the S^3, while the upper boundary, $\theta = \pi$ corresponds to the southpole. In this review we work with $\xi = e^{\psi_\xi} = 1$, so that the interface carries no F1 charge. This figure is adapted from [1, 2].

4.4 D3 Interface

The material of this section is found in great detail in [2]. Its S-dual is also found in [1].

A D3 interface is obtained by modifying (4.11d) by

$$\delta U^{D3} = -\frac{q^{\mathcal{D}}_{D3}}{2} \log\left(\frac{z-w}{z-\bar{w}}\right), \tag{4.23a}$$

$$\delta u^{D3} = -\frac{q^{\mathcal{D}}_{D3}}{2} \log\left|\frac{z-w}{z-\bar{w}}\right|^2, \tag{4.23b}$$

$$\delta \tilde{u}^{D3} = i\frac{q^{\mathcal{D}}_{D3}}{2} \log\left[\frac{(z-w)(\bar{z}-w)}{(z-\bar{w})(\bar{z}-\bar{w})}\right] \tag{4.23c}$$

where $w = R\, e^{i\Theta}$ with $R > 0$ and $\Theta \in (0, \pi)$. This produces a singularity in the interior of Σ. This is depicted in strip coordinates in figure 9 and in $\mathrm{AdS}_3 \times \mathrm{S}^3$ in figure 10. Again, this type of interface is smeared over the T_4 directions.

The interface carries a D3 brane charge,

$$Q^{\mathcal{D}}_{D3} = \pi\, q^{\mathcal{D}}_{D3}, \qquad q^{\mathcal{D}}_{D3} = \frac{(2\pi)^4 \alpha'^2}{\pi} N_3\,. \tag{4.24}$$

We mostly use the rescaled interface charge $q^{\mathcal{D}}_{D3}$; it is constrained to be positive. The second equation contains the integer-valued D3-brane charge N_3. This is the same normalization as in the D1/D5 case.

This D3 brane harbors one-brane charge. Indeed, the value of R plays a part in the F1 charge dissolved on the D3, and in order to suppress it, $R = 1$ needs to be chosen [1, 2]. This is the case, we focus on in this review. The D1 charge of the D3 interface is, on the other hand, given by

$$q^{\mathcal{D}}_{D1} \equiv -q^{(0)}_{D1} - q^{(\infty)}_{D1} = -q^{\mathcal{D}}_{D3} \Theta\, q_{NS5}, \tag{4.25}$$

As in the previous section, because the brane carries no F1 charge, by charge conservation the asymptotic regions have still the same central charge as in the vacuum solution, $\mathsf{c} =$

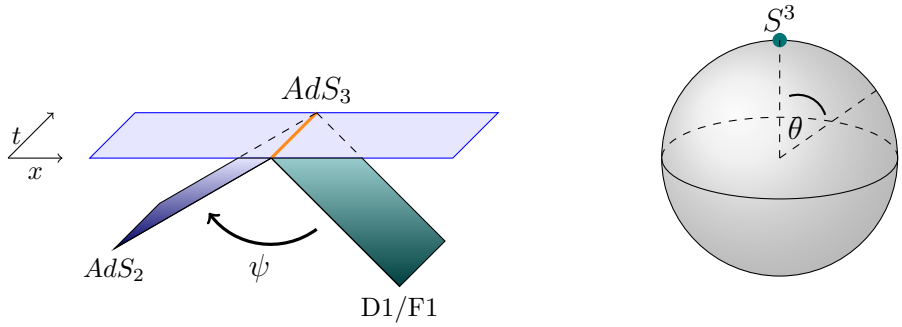

Figure 8: In coordinates $z = \exp(\psi + i\theta)$ AdS_3 is foliated by AdS_2 sheets shaded in dark blue and labeled by ψ. A D1/F1 string, shaded in green, is embedded into $AdS_3 \times S^3$ at $\xi = \exp \psi_\xi$, i.e. it sits at the north pole of S^3. The boundary of AdS_3, shaded in light blue, harbors the CFT and its intersection with the brane is the wordline of the field theory defect, colored in orange. This figure is adapted from [1, 2]. (For interpretation of the references to color in this figure legend, the reader is referred to the web version of this article [https://jhap.du.ac.ir/].)

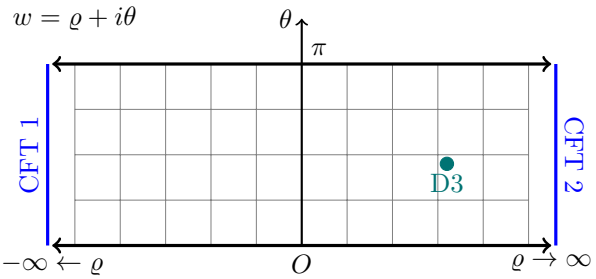

Figure 9: In contrast to the one-brane defect of the previous section, the D3 brane (green) defect is located in the interior of Σ at $w = \psi_R + \Theta$, with $R = e^{\psi}_R$. Hence the defect is no longer located at the poles of the S^3, but wraps an S^2 at some constant value Θ. This figure is adapted from [1, 2].

$6N_1N_5$. However, the asymptotic values of the RR four-form are affected

$$C_K(0) = -q^{\mathcal{D}}_{D3}\Theta = \frac{q^{\mathcal{D}}_{D1}}{q_{NS5}}, \qquad C_K(\infty) = 0. \tag{4.26}$$

This is why the brane cannot be a defect, but is rather an interface. Similar to the D1 interface, the dilaton remains the same at both asymptotic regions[16], c.f. (4.19) and the axion vanishes at both asymptotic regions.

It is convenient to define an effective, or "screened", D1 charge

$$q^{\Theta}_{D1} \equiv q^{\mathcal{D}}_{D1} \frac{\sin\Theta}{\Theta} \tag{4.27}$$

As before, the F1 and NS5 charges coincide at both asymptotic regions their superscripts can be dropped, $q_{F1} \equiv q^{(0)}_{F1} = -q^{(\infty)}_{F1} = \overline{q_{F1}}$ and $q_{NS5} \equiv q^{(0)}_{NS5} = -q^{(\infty)}_{NS5} = \overline{q_{NS5}}$. Similar to the

[16]The dilaton does differ at the asymptotic regions, when the interface carries F1 charge.

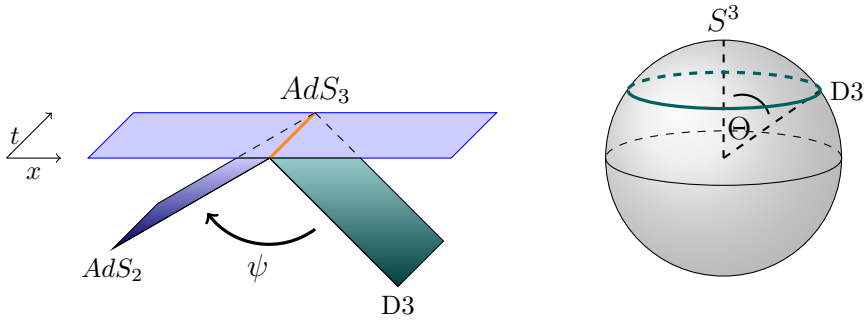

Figure 10: In coordinates $z = \exp(\psi + i\theta)$ AdS_3 is foliated by AdS_2 sheets shaded in dark blue and labeled by ψ. A D3 brane, shaded in teal, is embedded into $AdS_3 \times S^3$ at $w = \exp(\psi_R + i\Theta)$, i.e. it wraps an S^2 on the S^3. The boundary of AdS_3, shaded in light blue, harbors the CFT and its intersection with the brane is the wordline of the field theory defect, colored in orange. This figure is adapted from [1, 2]. (For interpretation of the references to color in this figure legend, the reader is referred to the web version of this article.)

vacuum solution, the D3 interface is determined by a set of holomorphic functions (4.11), where (4.11d) is now modified by (4.23). The parameters are

$$\nu = \frac{1}{2}\sqrt{\frac{q_{NS5}\, q_{F1}}{\kappa_0^{(\Theta)}}}, \quad \alpha = \frac{1}{2\sqrt{\kappa_0^{(\Theta)}}} e^{-\phi(0)}, \quad \eta = \frac{1}{2\sqrt{\kappa_0^{(\Theta)}}} \frac{q_{NS5}}{q_{F1}} e^{\phi(0)}, \quad \Theta = \frac{1}{q_{NS5}} \frac{q^{\mathcal{D}}_{D1}}{q^{\mathcal{D}}_{D3}} \tag{4.28}$$

where

$$\kappa_0^{(\Theta)} = \frac{T_{(4q_{F1},\, q^{\Theta}_{D1})} + T_{(0,\, q^{\Theta}_{D1})}}{T_{(4q_{F1},\, q^{\Theta}_{D1})} - T_{(0,\, q^{\Theta}_{D1})}}. \tag{4.29}$$

Note that the (p, q)-string tension, c.f. (4.22), is similar to that in (4.21), but with $q^{\mathcal{D}}_{D1}$ replaced by the screened charge q^{Θ}_{D1}. As in all previous solution, the parameter β is given by $\beta^2 = \alpha\eta$.

Observe that there are now two ways of turning off the interface's effective D1 charge off, $q^{\Theta}_{D1} = 0$. As before, there is the simple option $q^{\mathcal{D}}_{D1} = 0$. Additionally, we have now the option to set $\Theta = \pi$, for which the triple (ν, α, η) reduce to those of the vacuum solution, (4.13). As is discussed below in section 4.6, this case is much more subtle and interesting; in fact, the interface does not vanish entirely.

4.5 Solution Matching: the RG flow

So far, we described supergravity solutions for an F1/NS5 system harboring an extra D1 or D3 interface. Both solutions exist independently of each other. In this section, we connect these solutions by interpreting them as endpoints of an RG flow $D1 \to D3$. In fact, we establish that these are the Kondo-like flows (3.2), where the number of branes p is identified with $q^{\mathcal{D}}_{D1}$.

In the field theory, the RG flow is one of interfaces implying that the ambient CFTs remain unchanged. The ambient CFTs are characterized by the gauge rank $N_5 \propto q_{NS5}$, the central charge $\mathsf{c} \propto q_{NS5} q_{F1}$ and the dilaton ϕ, all of which remain unaffected by the interface RG flow,

$$Q^{\mathrm{IR}}_{brane} \stackrel{!}{=} Q^{\mathrm{UV}}_{brane}, \qquad \phi^{\mathrm{IR}} \stackrel{!}{=} \phi^{\mathrm{UV}}. \tag{4.30}$$

These expressions refer to the values at either asymptotic region. The UV solution is the D1 interface of section 4.3 and the IR corresponds to the D3 interface discussed in subsection 4.4.

We start by matching the D1 charge $q^{\mathcal{D}}_{D1}$ of both solutions. Identifying (4.17) and (4.25) yields

$$q^{\mathcal{D}}_{D3}\Theta = c. \tag{4.31}$$

For small Θ the D3 modification (4.23) reduces to the one-brane modification (4.16), $\delta U^{D3} \simeq \delta U^{F1}$, since $\xi = R = 1$[17] But also for finite Θ, i.e. after the flow is tripped, the three-brane interface occupies the same AdS_2 sheet as the one-brane interface did, namely that of smallest size, $x = 1$ ($\psi_\xi = 0$) and $R = 1$ ($\psi_R = 0$). The interface only moves inside of AdS_3 when $q^{\mathcal{D}}_{F1} \neq 0$ [1, 2].

Given the expressions (4.21) and (4.29) we can bound

$$1 \leq \frac{\kappa_0}{\kappa_0^{(\Theta)}} \leq \left(\frac{\Theta}{\sin\Theta}\right)^2, \tag{4.32}$$

which saturates for $\Theta = 0$. Moreover, through comparison of (4.20) and (4.28) we can express the triple $(\alpha^{\mathrm{IR}}, \eta^{\mathrm{IR}}, \nu^{\mathrm{IR}})$ through their analogs in the D1 interface

$$\nu^{\mathrm{IR}} = \sqrt{\frac{\kappa_0}{\kappa_0^{(\Theta)}}}\,\nu^{\mathrm{UV}}, \qquad \alpha^{\mathrm{IR}} = \sqrt{\frac{\kappa_0}{\kappa_0^{(\Theta)}}}\,\alpha^{\mathrm{UV}}, \qquad \eta^{\mathrm{IR}} = \sqrt{\frac{\kappa_0}{\kappa_0^{(\Theta)}}}\,\eta^{\mathrm{UV}}. \tag{4.33}$$

Our probe brane discussion that the angle Θ indicates the endpoint of the flow. This information is already encoded in the last equation of (4.28), where now the interface D1 charge derives from the UV configuration,

$$\Theta = \frac{1}{q_{NS5}}\frac{q^{\mathcal{D},\mathrm{UV}}_{D1}}{q^{\mathcal{D},\mathrm{IR}}_{D3}} = \frac{\pi}{N_5}\frac{p}{N_3}. \tag{4.34}$$

Here, the integer valued charges (4.15) and (4.24) were employed, and we returned to the notation of the last chapter for the interface charge, $q^{\mathcal{D},\mathrm{UV}}_{D1} = p$.

In our discussion leading up to (3.12), only a single D3 brane was incorporated in the description, $N_3 = 1$. Here, it becomes clear that the ration of D1 and D3 charge quantifies the value of Θ. In the following, we settle for $N_3 = 1$, however. Furthermore, the level of the $\hat{\mathfrak{su}}(2)_k$ WZW model, is given by the magnetic flux through the S^3, which is $N_5 = k$. Together this provides

$$\Theta = \frac{\pi p}{k} = \theta_p\,, \tag{4.35}$$

exactly as desired.

This confirms that the supergravity solutions studied in this section indeed correspond to the flows worked out in section 3. That is, the UV interface charge is dissolved into the D3 interface in the IR. Furthermore, the more units of D1 charge is dissolved into a single D3-brane, the further down the D3-branes slide on the S^3. This is in exact analogy with the mechanism in the original Kondo effect described in section 2.3.

When Θ is small, the D3 solution (4.28) is rather a one-brane interface (4.20). In the RG flow picture, this means that it is not energetically favorable for the interface to puff up from a stack of D1-branes into a (stack of) D3-brane. In other words, the UV interface does not possess enough charge to stabilize at a macroscopically visible two-sphere on the S^3. There is basically no RG flow.

[17] This also holds for arbitrary F1 charge on the interface, as long as $\xi = R$ is fixed.

4.6 Critical Screening

Now that a description of the fixed points is at our disposal, we can classify the flows according to three types outlined in section 2.2.2. To this end, the parameters of said section need to be translated to the language used in the present section, i.e. $2\mathsf{s} \to \frac{p}{N_3}$ and $k \to N_5$.

Over-screening occurs whenever the interface has not slid down all the way to the south pole of the S^3, i.e. the brane is an $S^2 \subset S^3$. This happens when $\frac{p}{N_3} < N_5$. Obviously, this happens most of the time in our holographic setup. Under-screening, on the other hand, which happens when $\frac{p}{N_3} > N_5$, is not described by our holographic flows. In this subsection, we turn to the critical case $\Theta = \pi$, which occurs when $p/N_3 = N_5$. This is the case occurring by default in the original Kondo problem, based on the WZW model $\hat{\mathfrak{su}}(2)_1$, and it describes the exact screening of the impurity by the conduction electrons. Its holographic pendant turns out to be subtle, yet surprisingly interesting! W.l.o.g. we choose $N_3 = 1$.

Observe that the modification to U in (4.23) vanishes when $w \in \partial\Sigma$, i.e. $\Theta = \pi$ and $\Theta = 0$. Therefore, the geometry should reduce to a pure F1/NS5 geometry in this limit. Using $q_{F1}^{\Theta=\pi} = 0$ and thus $\kappa_0^{(\Theta=\pi)} = 1$, it is easy to confirm from (4.28) that this is indeed the case.

This would be the end of the story if we ignored the RR 4-form potential, which according to (4.26) has a finite jump across the interface. Expressed through the Regge slope, this is

$$C_K(0) = 0 \quad \text{vs.} \quad C_K(\infty) = -(2\pi)^4 \alpha'^2 \,. \tag{4.36}$$

This puzzle derives from the circumstance that the modification (4.23) is not globally defined. After all, encircling the D3-brane once induces a finite shift in the value of C_K. In order to return it to its original value, a large gauge transformation must be performed. In this section, we argue that this realizes a duality transformation.

The tension with (4.26) can be seen to arise as follows. When comparing field values in the two asymptotic regions, their values need to be followed along a contour stretching from one asymptotic region to the other. This is illustrated for the UV solution in the left-hand diagram of figure 11. The asymptotic value of C_K on the right of the interface is determined by the interface's D1 charge p. In contrast to the D3 solution, the D1 solution (4.16) has no monodromies and is therefore globally defined. This implies that any other choice of $\mathcal{C}_1$ yields the same description.

When the RG flow is tripped, the D1-brane puffs up into a D3-brane characterized by the logarithms of (4.23). Due to the monodromy a different choice of contour results in a different description of the CFTs in each asymptotic region, as drawn in the center picture of figure 11. While $\mathcal{C}_1$ is as before, $\mathcal{C}_2$ gives a description in which the CFT at its end carries D1 charge $p - N_5$ rather than p.

These considerations are valid for any p. Setting $p = N_5$, i.e. $\Theta = \pi$, implies that the interface flows all the way to the upper boundary of Σ, squeezing $\mathcal{C}_1$ in the process. The asymptotic values (4.36) employ the contour $\mathcal{C}_1$. This is precisely the shift in C_K obtained under one of the parabolic generators of the extended U-duality group of IIB on T^4. In this frame, the interface starts out in the UV as a non-trivial interface joining two CFTs which are dual, and flows in the IR to a duality interface. In contrast, choosing $\mathcal{C}_2$, the interface can approach the upper boundary unhindered. Since the CFT on the right carries no D1 charge in this description, the interface must be the trivial interface. This is depicted in the right-hand diagram of figure 11. We have arrived at a holographic analog of critical screening in the Kondo model, where the ambient degrees of freedom screen the impurity completely.

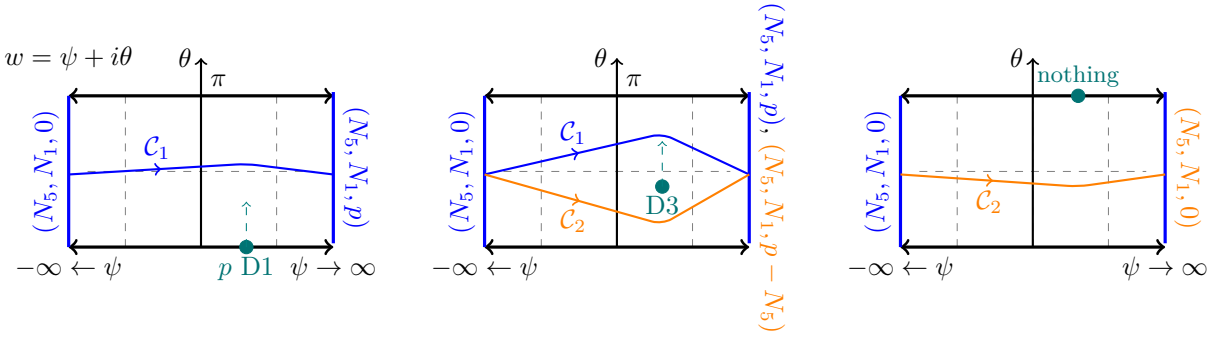

Figure 11: Left: When comparing fields between the two asymptotic regions contour $\mathcal{C}_1$ is followed. The interface charge is absorbed by the CFT on the right. Middle: Contour $\mathcal{C}_2$ defines another duality frame for the fields for which the right CFT carries no D1 charge. Right: In the frame $\mathcal{C}_2$ the interface flows all the way to the south pole, where it turns into the trivial interface. This figure is adapted from [1]. (For interpretation of the references to color in this figure legend, the reader is referred to the web version of this article [https://jhap.du.ac.ir/].)

5 Interface Entropies

As final act in this review, before concluding, we compute the interface entropy S_{imp}. It is the system size independent, i.e. non-extensive, contribution of the impurity to the full entropy of the system, and therefore it counts the interface degrees of freedom. It is convenient for us to work in terms of the so-called g-*factor*, given by $\mathsf{g} = e^{S_{\text{imp}}}$.

To develop an intuition for what to expect in our holographic model, we recall the original Kondo model. In the UV the system consists of free electrons and a decoupled impurity. In this case, the g-factor simply counts the spin states of the impurity, namely, it is the logarithm of the dimension of the impurity's representation [12]. In the IR, S_{imp} depends on the type of screening. For exact screening it vanishes, confirming that the impurity has "dissapeared". In the case of over-screening, S_{imp} takes a finite value in the IR. In all cases relevant to the Kondo model, it was observed in [12] that the number of degrees of freedom decreases along the RG-flow, i.e.

$$\lim_{T\to\infty} S_{\text{imp}} > \lim_{T\to 0} S_{\text{imp}} \tag{5.1}$$

In fact, it was later shown in [51] that this is a general characteristic of any boundary RG flow in $(1+1)$-dimensional CFT. This is known as the g-*theorem*.

For our holographic RG flows, two different frameworks lie at our disposal to compute the g-factor. The backreacted supergravity solutions of the previous section and the probe branes in the section before that. By computing the g-factor in both pictures, we elucidate the importance of backreaction. Taking a step further, we confirm the validity of the g-theorem for our flows, thus legitimating their existence fully. The analysis presented here appeared before in [2] and its analog in the D1/D5 system was discussed in [1].

The interface entropy is defined through its boundary analog via the folding trick. The *boundary entropy*, or g-*factor* is defined as follows [12]. Place the CFT on a cylinder of radius r and length ℓ, with boundary states $\|\alpha\rangle\rangle$ and $\langle\langle\alpha\|$ delimiting it. In the limit $\ell \gg r$

the partition function of a unitary BCFT has the expansion

$$\log Z = \frac{\pi \mathsf{c}}{6}\frac{\ell}{r} + s_\alpha + O(r/\ell) \tag{5.2}$$

where s_α depends only on $\|\alpha\rangle\rangle$ and stands in relation to the g-factor through $g_\alpha = e^{s_\alpha}$, hence $s_\alpha = S_{\text{imp}}$.

It was demonstrated in [53] that the g-factor can be extracted from the entanglement entropy if the entangling interval of length ζ_0 is anchored at the boundary. Then

$$S_{\zeta_0} = \frac{\mathsf{c}}{6}\log\frac{\zeta_0}{\epsilon} + s_{\mathcal{A}} + O(\epsilon)\,, \tag{5.3}$$

with central charge c, UV-cutoff ϵ, and conformal boundary condition α. Interfaces may be thought of as unfolded BCFTs with central charge $\mathsf{c} = \mathsf{c}^{(0)} + \mathsf{c}^{(\infty)}$. Since the fold is the locus of the interface, the entanglement interval reaches symmetrically into both sides of the interface.

We begin in section 5.1 by explaining how the interface entropy is extracted from the supergravity solutions of [49]. Thereafter, in section 5.2, we apply this technique to the backreacted supergravity solutions of the previous section and discuss the g-theorem. As before, we present the F1/NS5 scenario. However, the probe brane limit is performed easiest in the D1/D5 frame. Therefore, we S-dualize before describing the probe brane limit. Crucially, this confirms that the supergravity solution contains more information than the probe brane picture.

5.1 Interface Entropy in Asymptotically $\mathrm{AdS}_3 \times S^3$ Solutions

In this subsection, all relevant ingredients for the computation of g-factors from the supergravity solutions in questions are provided. The formalism provided here was derived in [55] and the reader is referred to that source for a detailed account.

The starting point of the discussion is (5.3), leading to the question of computing entanglement entropy in gravity. Famously, an answer has been given by Ryu and Takayanagi (RT) when dealing with holographic CFTs. For an entanglement region $\mathcal{A}$, they propose [54] that the entanglement entropy in a d-dimensional CFT is given as area of a minimal surface $\gamma_{\mathcal{A}}$ reaching into the bulk of AdS_{d+1} and anchored to $\mathcal{A}$,

$$S_{\mathcal{A}} = \frac{\mathrm{Area}(\gamma_{\mathcal{A}})}{4G_N}. \tag{5.4}$$

Newton's constant G_N belongs, in our case, to the ten-dimensional spacetime into which the minimal area surface is embedded. Usually the minimal surface has codimension-2 making it eight-dimensional here.

Recall the Janus coordinates used in (4.14). Using Poincaré patch coordinates (ζ, t) on a single AdS_2 and $r = e^{\psi}$ an asymptotic region in AdS_3, say $r \to 0$, has the metric

$$ds^2_{\mathrm{AdS}_3} = \mathsf{L}^2\left(\frac{dr^2}{r^2} + \frac{\mu}{4}\frac{1}{r^2}\frac{d\zeta^2 - dt^2}{\zeta^2}\right). \tag{5.5}$$

This particular AdS_2 sheet approaches one half of the CFT spacetime and (ζ, t) are identified with the CFT coordinates on that side. For the vacuum geometry (4.14) the extra factor μ is one. Should an interface be present, however, then $\mu \neq 1$. In general, each asymptotic region has its own μ, so that, similar to the charges, a label is ascribed, $\mu^{(0)}$ or $\mu^{(\infty)}$.

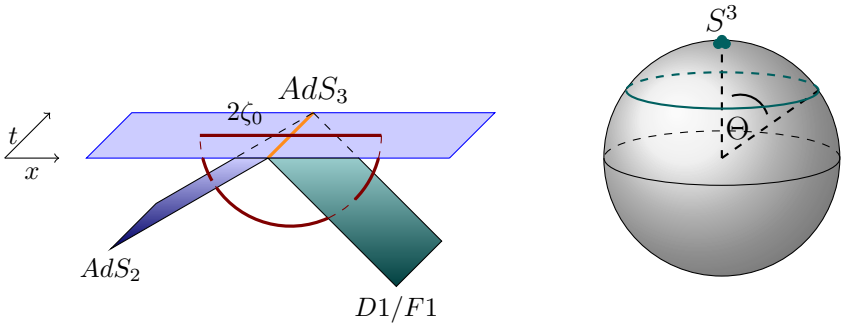

Figure 12: Entanglement minimal surface is depicted in red and wraps all of S^3 (and T^4) and is a geodesic inside AdS_3 anchored at a CFT space interval of size $2\zeta_0$. As before the impurity interface is drawn in teal. On the S^3, the dots are understood as UV impurity and the circle (really an S^2) as the IR impurity. In the case studied in this review, the impurity carries only D1 charge and therefore hangs down orthogonal to the boundary as in figure 5. This figure is adapted from [1,2]. (For interpretation of the references to color in this figure legend, the reader is referred to the web version of this article.)

One boundary of the entanglement interval is placed at a distance ζ_0 from the interface locus ($\zeta = 0$). The entanglement interval extends an equal distance to the other side of the interface so that its size is $\mathcal{A} = 2\zeta_0$. This is depicted in figure 12. Fixing time, the minimal area surface $\gamma_{\mathcal{A}}$ pierces each AdS_2 sheet at the same value of the spatial coordinate $z = z_0$. This is synonymous with the entangling interval lying symmetrically about the interface. Recall that this requirement follows from the folding trick, as explained above.

Putting everything together, γ_A wraps $S^2 \times T_4 \times \Sigma$ and is a geodesic inside of AdS_3. The pulled back metric has $ds^2_{AdS_2} = 0$ so that

$$S_{\mathcal{A}} = \frac{1}{4G_N^{(10)}} \int_{S^2} d\Omega_2 \int_{T^4} d\Omega_4 \int_{\Sigma} \rho^2 \, f_2^2 \, f_3^4. \tag{5.6}$$

Here, $d\Omega_2$ and $d\Omega_4$ are the volume elements of unit radii for $S^2$and T^4, respectively. They can be integrated over trivially since the metric functions depend only on the coordinates of Σ. Given the general form of the metric factors (4.2a)-(4.2d) the minimal area of $\gamma_{\mathcal{A}}$ becomes

$$S_{\mathcal{A}} = \frac{\mathrm{Vol}(S^2)}{4G_N^{(10)}} \int_{\Sigma} (a\,u - b^2) \left| \frac{\partial_z V}{B} \right|^2. \tag{5.7}$$

This integral is divergent, as expected of a boundary anchored geodesic in AdS_3. In coordinates $z = re^{i\theta}$ on Σ, the cutoffs at $r \to 0$ and $r \to \infty$ are given by

$$r_\infty = \frac{2\zeta_0}{\epsilon\sqrt{\mu^{(\infty)}}}, \qquad r_0^{-1} = \frac{2\zeta_0}{\epsilon\sqrt{\mu^{(0)}}}, \tag{5.8}$$

where ϵ is the UV cutoff in the CFT. Since $\mu^{(0)}$ and $\mu^{(\infty)}$ are different in general, the cutoffs are a priori distinct for both asymptotic regions. In our case they will coincide, however. This ends our recapitulation of [55].

5.2 D1 and D3 Interface Entropy

Now that a formalism for the computation of the interface entropy is at hand, we apply it in this subsection to the D1 and D3 solutions of the previous section. Thereafter, in order to take the probe brane limit, the resulting interface entropies are S-dualized into the D1/D5 frame.

The following abbreviations come in handy,

$$q_{F1}^{bare} = 4\nu\sqrt{\alpha\eta} = \begin{cases} \frac{q_{F1}}{\kappa}, & \text{UV}, \\ \frac{q_{F1}}{\kappa^{(\Theta)}}, & \text{IR}, \end{cases} \tag{5.9}$$

The charge q_{F1}^{bare} would be the F1 charge, were it not for the modifications (4.16) and (4.23), as can be seen by recalling (4.12). By itself, it is not a Page charge in the interface solutions and thus changes under the RG flow. Therefore, it is no physical charge in the cases of interest, but rather a bookkeeping device.

Another important ingredient are the scale factors $\mu^{(0,\infty)}$, which contribute to (5.1). As derived in detail in [2] for the cases of interest here, these scale factors coincide at both asymptotic regions and are given by

$$\mu^{(0)} = \mu^{(\infty)} = \begin{cases} \frac{1}{\kappa}, & \text{UV}, \\ \frac{1}{\kappa^{(\Theta)}}, & \text{IR}, \end{cases} \tag{5.10}$$

where the reader is reminded of (4.21) and (4.29). We can now proceed to compute the interface entropy.

Because $u = u_0 + \delta u$ the entanglement entropy is computed in two steps. First we tend to the contribution from the vacuum background stemming from u_0 into which the interfaces are embedded,

$$\begin{aligned} \mathcal{I}_0 =& \operatorname{Vol}(S^2) \int_\Sigma (a\, u_0 - b^2) \left| \frac{\partial_z V}{B} \right|^2 \\ =& 4 \operatorname{Vol}(S^3)\, q_{NS5}\, q_{F1}^{bare} \log \frac{r_\infty}{r_0} \end{aligned} \tag{5.11}$$

The second part is provided by the interface deformations, (4.16) and (4.23), respectively,

$$\mathcal{I}_{\text{UV, IR}} = \operatorname{Vol}(S^2) \int_\Sigma a\, \delta u^{D1,\,D3} \left| \frac{\partial_z V}{B} \right|^2 . \tag{5.12}$$

This becomes

$$\mathcal{I}_{\text{UV}} = 4 \operatorname{Vol}(S^3)\, q_{NS5} \left[-\left(-q_{F1} + q_{F1}^{bare,\text{UV}} \right) \log r_\infty + \left(q_{F1} - q_{F1}^{bare,\text{UV}} \right) \log \frac{1}{r_0} + q_{F1} - q_{F1}^{bare,\,\text{UV}} \right], \tag{5.13a}$$

$$\mathcal{I}_{\text{IR}} = 4 \operatorname{Vol}(S^3)\, q_{NS5} \left[-\left(-q_{F1} + q_{F1}^{bare,\text{IR}} \right) \log r_\infty + \left(q_{F1} - q_{F1}^{bare,\text{IR}} \right) \log \frac{1}{r_0} + q_{F1} - q_{F1}^{bare,\,\text{IR}} \right]. \tag{5.13b}$$

Combining this with (5.11) as well as employing (5.1), (5.9), (5.10) and the relation (4.10) for the central charges, what results is

$$S_{2\zeta_0}^{\text{UV, IR}} = \frac{\mathcal{I}_0 + \mathcal{I}_{\text{UV, IR}}}{4G_N^{(10)}} = \frac{\mathsf{c}^{(\infty)} + \mathsf{c}^{(0)}}{6} \log \frac{2\zeta_0}{\epsilon} + \log \mathsf{g}^{\text{UV, IR}}. \tag{5.14}$$

Of course, the central charges coincide at both sides of the interface. Writing the result in this way illustrates that the entanglement entropy assumes the desired form of a BCFT (5.3), with combined central charges. The g-factors are

$$\log \mathsf{g}^{UV} = \frac{\mathsf{c}^{(\infty)} + \mathsf{c}^{(0)}}{12}\left(\log \kappa + 1 - \frac{1}{\kappa}\right), \tag{5.15a}$$

$$\log \mathsf{g}^{IR} = \frac{\mathsf{c}^{(\infty)} + \mathsf{c}^{(0)}}{12}\left(\log \kappa^{(\Theta)} + 1 - \frac{1}{\kappa^{(\Theta)}}\right), \tag{5.15b}$$

If $q^{\mathcal{P}}_{D1} \to 0$ it follows that $\kappa \to 1$ and $\kappa^{(\Theta)} \to 1$. Therefore, both g-factors vanish confirming that there are no degrees of freedom on the interface, as expected since the geometries reduce to the vacuum, or trivial interface, in this limit.

We can now turn to the g-theorem, i.e. the decreasing of the g-factor along the RG flow in a two-dimensional CFT. This is most easily confirmed by considering the difference between the boundary entropies,

$$\log \frac{\mathsf{g}^{UV}}{\mathsf{g}^{IR}} = \frac{\mathsf{c}^{(\infty)} + \mathsf{c}^{(0)}}{12}\left(\log \frac{\kappa}{\kappa^{(\Theta)}} + \frac{1}{\kappa^{(\Theta)}} - \frac{1}{\kappa}\right) \tag{5.16}$$

By virtue of the lower bound in (4.32) this expression is always non-negative. Hence, the g-theorem is satisfied, thereby fully legitimating the existence of our Kondo flows, even with strong backreaction!

Of course, (5.16) vanishes for $\Theta = 0$, since $\kappa^{(0)} = \kappa$ meaning that the D3 interface simply reduces to the stack of D1 interfaces. More interestingly, for the case of critical screening, i.e. $\Theta = \theta_p = \pi$, the g-factor, (5.15b), vanishes in the IR. This is in line with our interpretation that the interface implements a duality transformation. Furthermore, the vanishing of the g-factor in the case of critical screening parallels the original Kondo problem.

Boundary Entropy in D1/D5 System

In order to reach the probe brane limit, it is convenient to move to the D1/D5 frame, which is achieved via S-duality. In the solutions at hand, this is implemented by [64]

$$S: \qquad \begin{pmatrix} q_{D1} \\ q_{F1} \end{pmatrix} \to \begin{pmatrix} 0 & 1 \\ -1 & 0 \end{pmatrix} \begin{pmatrix} q_{D1} \\ q_{F1} \end{pmatrix}, \tag{5.17}$$

$$\begin{pmatrix} q_{D5} \\ q_{NS5} \end{pmatrix} \to \begin{pmatrix} 0 & 1 \\ -1 & 0 \end{pmatrix} \begin{pmatrix} q_{D5} \\ q_{NS5} \end{pmatrix} \tag{5.18}$$

The D3 charge q_{D3} is invariant under S-duality. On the fields, S acts through

$$S: \qquad C_K \to C_K, \qquad f_3^4 \to f_3^4, \qquad \tau \to -\frac{1}{\tau}, \tag{5.19}$$

where $\tau = \chi + ie^{-\phi}$. In all of our solutions, the axion χ vanishes at the asymptotic regions. Therefore, the last transformation simply flips the sign of the dilaton, $e^{\phi(0)} \to e^{-\phi(0)}$, as it should. Applying S-duality to (5.15) readily yields the g-factors in the D1/D5 frame,

$$\log \mathsf{g}_S^{UV} = \frac{\mathsf{c}_S^{(\infty)} + \mathsf{c}_S^{(0)}}{12}\left(\log \kappa_S + 1 - \frac{1}{\kappa_S}\right), \tag{5.20a}$$

$$\log \mathsf{g}_S^{IR} = \frac{\mathsf{c}_S^{(\infty)} + \mathsf{c}_S^{(0)}}{12}\left(\log \kappa_S^{(\Theta)} + 1 - \frac{1}{\kappa_S^{(\Theta)}}\right), \tag{5.20b}$$

where κ_S is found from (4.21) by swapping the labels F1 and D1 in the string tensions. In the same manner, $\kappa_S^{(\Theta)}$ derives from (4.29). The central charges are still $\mathsf{c}^{(0)} = \mathsf{c}^{(\infty)} = 6N_5N_1$, where N_5 is now the number of D5 branes and N_1 the number of D1 branes. The interface carries now F1 instead of D1 charge.

Probe Brane Limit

The probe brane limit is reached in the D1/D5 frame by having the dilaton shrink, i.e. an expansion of (5.20) for small dilaton $e^\phi \ll 1$ is required,

$$\log \mathsf{g}^{UV} = \frac{Q_{D5}Q_{F1}^{\mathcal{D}}}{4\pi\kappa_{10}^2}e^\phi + \mathcal{O}(e^{2\phi}) = N_5\, p\, e^\phi + \mathcal{O}(e^{2\phi}), \tag{5.21a}$$

$$\log \mathsf{g}^{IR} = \frac{Q_{D5}Q_{F1}^{\mathcal{D}}}{4\pi\kappa_{10}^2}\frac{\sin\Theta}{\Theta}e^\phi + \mathcal{O}(e^{2\phi}) = N_5\, p\, \frac{\sin\Theta}{\Theta}e^\phi + \mathcal{O}(e^{2\phi}). \tag{5.21b}$$

The reader is reminded that the dilaton coincides on both regions, (4.19). Evidently, the probe brane expression carries less information than the full supergravity result (5.20). Thus, important information on the amount of the interface degrees of freedom is encoded in gravitational backreaction.

The g-theorem is seen to be satisfied trivially,

$$\log \frac{\mathsf{g}^{UV}}{\mathsf{g}^{IR}} = N_5\, p \left(1 - \frac{\sin\Theta}{\Theta}\right) e^\phi + \ldots, \tag{5.22}$$

In the case that no flow occurs, $\Theta = 0$, this vanishes.

This demonstrates that the probe brane limit does not account for all degrees of freedom captured on the interface.

6 Conclusions and Outlook

A stack of pointlike branes condenses into a single spherical brane while sliding down on an S^3; that is the Kondo effect. This picture of the Kondo effect has been successfully implemented holographically in [1, 2]. Both of these sources considered impurities with D1 and F1 charge placed within the ten-dimensional geometry $AdS_3 \times S^3 \times M_4$, where M_4 is either T_4 or K_3. It is the purpose of this review to provide a beginners guide into the model by considering impurities of only one type of charge. Since this review works entirely in the F1/NS5 frame, the impurity carries D1 charge. In the D1/D5 frame, the impurity carries F1 charge.

This holographic model has a number of virtues. First of all, not only is the CFT Lagrangian known, it is also one of the best studied versions of the AdS/CFT correspondence. Second, comparing with the multi-channel Kondo model based on $SU(2)_k$, where the level k corresponds to the number of flavors, one can draw a comparison to the holographic flows discussed in this review. In this case, the S^3 factor has a description in terms of $SU(2)_{N_5}$, so that N_5 may be treated as the number of electron flavors. Third, the holographic Kondo flow preserves half of the supercharges of the fixed points. In fact, it is this property which granted the required control to derive the RG flow solutions, as demonstrated in section 3.3. Moreover, in [1] the κ-symmetry corresponding to the preserved supercharges is employed to derive the BPS flow equations for the entire class of (p, q)-string interfaces, of which only the D1 interface is treated in this review.

Two steps had to be taken to establish the flow. First, it was necessary to demonstrate the existence of a relevant perturbation in the UV theory. Using the non-abelian DBI action, it was seen in section 3.2 that such a perturbing operator indeed exists, and is in fact marginally relevant, just as in the Kondo model. Second, the flow was shown in section 3.3 to terminate at a non-trivial fixed point in the IR. The relevant techniques had already been employed in higher dimensions [62], and allowed us here to determine the flow profile of the polar angle θ on the S^3. The impurity brane resides on the same AdS_2 sheet along the entire flow for the case of a pure D1 interface. This changes if F1 charge is included. Readers interested in the flow profile of the AdS_2 sheet on which the impurity brane resides are referred to [1]. Altogether, this establishes the existence of the envisioned holographic Kondo-like flows.

The probe brane description is inherently limited since many quantities of interest rely on backreaction, such as correlators in the CFT or the g-factors. It is therefore not just worthwhile, but necessary to construct a geometry which incorporates the backreaction of the interface along the flow. This is a very difficult and ambitious task. The first steps in accomplishing it were taken in [1] for the D1/D5 frame and in [2] for the F1/NS5 system. Indeed, for these cases, the fully backreacted geometry for the flow fixed points were constructed using the general solution of [49]. In this review, only the simplest example in the F1/NS5 frame was presented, i.e. that of an impurity with pure D1 charge. The UV impurity was presented in section 4.3 and the IR impurity in section 4.4. They were set into relation with each other and shown to agree with the probe brane description in section 4.5. This allowed to discuss critical screening in section 4.6, which is not possible in the probe brane description. The impurity was demonstrated to become a duality interface in this limit.

As demonstrated in section 5, an important quantity for which backreaction is crucial is the boundary entropy, or g-factor. We reviewed their computation for the UV and IR fixed points for a pure D1 interface inside the F1/NS5 system, once with and without backreaction. The g-factors were shown to decrease from the UV to the IR, thereby confirmind the validity of the g-theorem and fully legitimating the existence of this class of Kondo-like RG flows. In the case of critical screening, the g-factors vanish in the IR, just as for the original Kondo model. In contrast to the original Kondo model, however, the interface becomes a duality interface in the IR for critical screening.

Outlook

The sources [1,2] considered a single impurity. An obvious extension is to include more than one impurity in the ambient system and follow through with the same program as before, i.e. demonstrating the existence of an RG flow and, if possible, find corresponding backreacted supergravity solutions of the fixed points. It is desirable to construct lattices of Kondo impurities, as those are relevant in experiment. Employing the Kondo-like impurities of this review has the immediate advantage that the systems is automatically strongly coupled by virtue of the AdS/CFT correspondence.

In the case of (only) two impurities, it is interesting to explore brane annihilation processes. To do so, a stack of pointlike branes is placed in the UV at the north pole and a similar stack of opposite charge at the south pole. The absolute value of the charges should be large enough for the puffed up branes to meet somewhere on the S^3 along the RG flow; this need not necessarily be the equator. Other directions lead to the computation of reflection and transmission coefficients of these interfaces [63,65], one- and two-point functions, or the inclusion of temperature via extra black holes in the gravity dual. The latter is particularly interesting as it would allow for comparisons with the original Kondo problem. One should

keep in mind though that, as constructed here, the energy scale is not temperature, but the radial coordinate of AdS_3.

Finally, there is interface-interface fusion or interface-boundary fusion [20], which can be studied explicitly in the gravity dual. Unfortunately, the interfaces discussed in this review are not chiral as required for the application of techniques in [20]. This is in fact one major difference compared with the original Kondo model, in which the interfaces are indeed chiral. A possible solution is therefore to repeat the program presented in this review in a different string theory background based on AdS_3, which have seen remarkable progress recently [66–77]. Natural candidates have a dual geometry with asymptotic $AdS_3 \times S^3 \times S^3 \times S^1$ regions, since they contain three-spheres on which to stage the Kondo flow. The main virtue of $AdS_3 \times S^3 \times S^3 \times S^1$ is that it features points in moduli space, where the CFT is described by cosets. This algebraic structure substantially increases the chances of finding chiral interfaces. These, in turn, make way to find fusion processes in gravity.

Acknowledgments

It is my pleasure to thank Johanna Erdmenger for carefully reading the draft of this review and for providing valuable input. I acknowledge support by the Deutsche Forschungsgemeinschaft (DFG, German Research Foundation) under Germany's Excellence Strategy through the Würzburg-Dresden Cluster of Excellence on Complexity and Topology in Quantum Matter -? ct.qmat (EXC 2147, project - id 390858490). I am furthermore supported via project id 258499086 - SFB 1170 'ToCoTronics'.

A Conformal Field Theory

This section presents the required toolkit from two dimensional CFT. The picture that arises from this CFT analysis is the one we intend to mimic in holography. Therefore, these concepts are important to keep in mind when working through the gravity computations of this review. However, the technical details are perhaps not so important, since the relevant techniques from CFT are not explicitly applied in the gravity setup. Therefore, this section is in nature more of a summary of relevant CFT ingredients rather than a careful introduction with detailed derivations. There are, however, several excellent references, from where we draw the material presented here, e.g. [57, 59, 78, 79].

Our discussion is geared towards understanding the boundary conditions in the $\hat{\mathfrak{su}}(2)_k$ WZW model. We begin with the description of its bulk CFT. Thereafter a brief survey of boundary conditions in of this model is presented in section A.2. Lastly, the concept of an interface CFT in $(1+1)$ dimensions is discussed in section A.3.

A.1 Conformal Field Theory on the Plane

In this review the set of all primaries in the theory is called I and its elements are tuples $(i, \bar{\imath})$, where i labels the holomorphic piece of the primary with conformal weight h_i and $\bar{\imath}$ labels the antiholomorphic piece with conformal weight $h_{\bar{\imath}}$. Primary states are denoted $|\phi_{i,\bar{\imath}}\rangle$.

In general, covariance of a quantum field theory under some symmetry algebra $\mathcal{W} \times \overline{\mathcal{W}}$ means that its spectrum carries an action of this algebra. In the case of CFT this is $\mathcal{W} = \mathsf{Vir}$ and $\overline{\mathcal{W}} = \overline{\mathsf{Vir}}$, which stands for the Virasoro algebra,

$$[L_n, L_m] = (n-m)L_{n+m} + \frac{\mathsf{c}}{12} n(n^2-1)\delta_{n+m,0} \tag{A.1}$$

with central charge c.

Given this situation, the state space consists of superselection sectors,

$$\mathcal{H} = \bigoplus_{(i,\bar{\imath})\in I} M_{i,\bar{\imath}}\, \mathcal{H}_i \otimes \mathcal{H}_{\bar{\imath}}, \tag{A.2}$$

where $\mathcal{H}_i$ and $\mathcal{H}_{\bar{\imath}}$ are irreducible representations of the conformal algebra. They are synonymous with conformal families. The matrix $M_{i,\bar{\imath}}$ counts the multiplicity of each primary field in the theory at hand. The presence of a unique conformally invariant vacuum state, labeled by $i = \bar{\imath} = 0$, is captured through $M_{0,0} = 1$. The partition function corresponding to this state space is

$$Z(\tau,\overline{\tau}) = \sum_{(i,\bar{\imath})\in I} M_{i,\bar{\imath}}\, \chi_i(q)\, \chi_{\bar{\imath}}(\overline{q}), \tag{A.3}$$

where $q = e^{2\pi i\tau}$ and $\overline{q}$ is its complex conjugate. The modular parameter τ is itself complex. The states coming from each individual representation $\mathcal{H}_i$ are counted by the *characters*,

$$\chi_i(q) = \mathrm{Tr}_{\mathcal{H}_i} q^{L_0 - \frac{c}{24}}. \tag{A.4}$$

A.1.1 Wess-Zumino-Witten Models

Wess-Zumino-Witten (WZW) possess an extended symmetry algebra containing the Virasoro algebra. The literature on them is vast and only the minimal elements required for this review are summarized here. Excellent introductions can be found in [57, 78, 80], which are all rooted in the seminal work [81].

The spectrum of Wess-Zumino-Witten models carries, additionally to $\mathsf{Vir}\times\overline{\mathsf{Vir}}$, an action of a *Kac-Moody algebra* $\hat{\mathfrak{g}}_k \times \bar{\hat{\mathfrak{g}}}_k$,

$$\left[J^a_n, J^b_m\right] = i f^{abc} J^c_{n+m} + k\, n\, \delta^{ab}\, \delta_{n,-m} \tag{A.5}$$

$$\left[\bar{J}^a_n, \bar{J}^b_m\right] = i f^{abc} \bar{J}^c_{n+m} + k\, n\, \delta^{ab}\, \delta_{n,-m} \tag{A.6}$$

$$\left[J^a_n, \bar{J}^b_m\right] = 0. \tag{A.7}$$

In the following we omit the antiholomorphic sector as the analysis is identical. Similar to the Virasoro algebra, a central element, k, is present. Note also the appearance of the structure constants f^{abc} of the underlying Lie algebra $\mathfrak{g}$ and thus a, b, c run over its adjoint representation. In fact, the Lie bracket of $\mathfrak{g}$ is recovered by fixing $n = m = 0$ in (A.5). The relation of the Kac-Moody modes to the Virasoro modes is

$$[L_n, J^a_m] = -m J^a_{n+m}. \tag{A.8}$$

The Kac-Moody generators can be collected as modes of current field with conformal weight one

$$J^a(z) = \sum_{n\in\mathbf{Z}} z^{-n-1} J^a_n \tag{A.9}$$

The energy-momentum tensor follows from the Sugawara construction,

$$T(z) = \frac{1}{2(k+g)} \sum_a \left(J^a J^a\right)(z). \tag{A.10}$$

Here, the parentheses enclosing the currents indicate a normal ordered product and g is the dual coxeter number. In the case of our interest, $\hat{su}(N)_k$ we have $g = N$.

Whenever an extended symmetry is present, it is sensible to classify the state space according to the highest weight states of the extended symmetry algebra, instead of the Virasoro algebra. A thorough analysis of the representation theory of affine Lie algebras is found in [57, 58]. Here, we contend ourselves with describing the case most relevant to the original Kondo problem, $\hat{\mathfrak{su}}(2)_k$. It has $k+1$ highest weight states also termed WZW primaries each labeled by a half integer $j = 0, \frac{1}{2}, 1, \dots \frac{k}{2}$, which carries the interpretation of spin. This model's partition function is

$$Z(\tau, \overline{\tau}) = \sum_{j=0}^{k/2} |\chi_j(\tau)|^2, \tag{A.11}$$

where the sum runs over half-integers. In this model the characters in the holomorphic and anti-holomorphic sector are complex conjugates of each other leading to the absolute value. Note that infinite amount of Virasoro primaries present in this theory is repackaged into a finite number of WZW primaries. All WZW primaries are also Virasoro primary, while the converse is not true.

A.1.2 Fusion Rules

Whenever representations are at hand, we may ask what their tensor products are, which should decompose into a sum of irreducible representations of the algebra, weighted by Clebsch-Gordan-type coefficients. In our case the representations are infinite dimensional and the regular tensor product develops unwanted properties. However, an appropriate tensor product can be defined [82, 83]. It is called the *fusion product*,

$$[\phi_i] \star [\phi_j] = \sum_k N_{ij}^k \, [\phi_k]. \tag{A.12}$$

Here, $[\phi_i]$ stands for a representation of the chiral algebra, which in the case of an Kac-Moody symmetry algebra corresponds to a WZW family. The integer coefficients N_{ij}^k, which are the analogue of the Clebsch-Gordan coefficients, are called *fusion rules*. They are symmetric in the lower two indices,

$$N_{ij}^k = N_{ji}^k \tag{A.13}$$

and satisfy an associativity relation

$$\sum_m N_{im}^l \, N_{jk}^m = \sum_n N_{ij}^n \, N_{nk}^l. \tag{A.14}$$

The vacuum representation $i = 0$ assumes the role of the unit element under fusion, $N_{0j}^k = \delta_{i,k}$, or equivalently $[\phi_0] \star [\phi_j] = [\phi_j]$. Moreover, the *conjugate representation* i^+ fuses with i into the unit element,

$$N_{ij}^0 = \delta_{j,i^+}. \tag{A.15}$$

The relevant algebra for the Kondo problem is $\hat{\mathfrak{su}}(2)_k$, for which each representation is its own conjugate, i.e., $N_{ii}^0 = 1$. The model's fusion rules are

$$N_{j_1 j_2}^{j_3} = \begin{cases} 1 & \text{if } |j_1 - j_2| \leq j_3 \leq \min(j_1 + j_2, k - j_1 - j_2) \text{ and } j_1 + j_2 + j_3 \in \mathbb{Z}, \\ 0 & \text{otherwise.} \end{cases} \tag{A.16}$$

where the j_i range within $0, \frac{1}{2}, 1, \dots, \frac{k}{2}$.

A.2 Boundary Conformal Field Theory

We are now set to confine a CFT to a system with boundaries. This program was single-handedly brought to life by Cardy in [84]. Many good reviews can be found [59, 85, 86]; we draw mainly from [59].

A.2.1 Gluing Conditions and Boundary Spectra

While ordinary CFT is defined on the entire complex plane, a BCFT is defined only on the upper half plane $\Im z \geq 0$, with a boundary condition α fixed along the real line. Translational invariance perpendicular to the boundary is broken and the requirement that neither energy nor momentum leak through the boundary to the lower half plane is secured by

$$T(z) = \overline{T}(\overline{z}) \quad \text{for } z = \overline{z}. \tag{A.17}$$

Relations, which relate holomorphic to antiholomorphic fields at the boundary are called *gluing conditions*. Any boundary condition α which respects (A.17) is a *conformal boundary condition*. Recall that CFTs on the entire plane are governed by two independent copies of the Virasoro algebra. Introducing a boundary relates the two copies via (A.17), so that the theory carries an action of only a single Virasoro algebra. Similarly, in the case of extended symmetries, only a single copy of the algebra acts on the theory. This is perhaps the most striking difference with CFTs without boundaries. Thus the spectrum is no longer bilinear in representations of the chiral algebra, c.f. (A.2), but only linear

$$\mathcal{H}_\alpha = \bigoplus_i \mathcal{H}_i^{n_\alpha^i}, \tag{A.18}$$

where i labels again representations of the chiral algebra and α a conformal boundary condition. The integers n_α^i account for possible multiplicities of one representation.

Extended symmetries are also glued along the boundary $\Im z = 0$. In the case of a Kac-Moody algebra conformal boundary conditions allow for an additional local automorphism Ω of $\hat{\mathfrak{g}}_k$ in the gluings of the currents,

$$J(z) = \Omega[\overline{J}(\overline{z})] \quad \text{for } z = \overline{z}, \tag{A.19}$$

so long as we respect (A.17), i.e. $\Omega[T] = T$.

We stick here to $\Omega = \mathbf{1}$, known as the *Cardy case* [84]. In this case, the set of boundary conditions is in one-to-one correspondence with the allowed primaries in the theory. Hence the conformal boundary conditions are labeled by the set of primaries I, i.e., $\alpha = i$. Furthermore, Cardy managed to show that the multiplicities in (A.18) are in fact the fusion rules $n_\alpha^i \equiv n_j^i = N_{jj}^i$. Therefore, partition function of the theory is

$$Z_{\alpha=j}(\tau) = \sum_{i \in I_{\mathcal{W}}} N_{jj}^i \, \chi_i(\tau)\,. \tag{A.20}$$

The subscript on Z declares, which boundary condition is placed along the real line.

A.2.2 An Example Relevant in the Kondo Model

Returning to the model of interest in the Kondo problem, $\hat{\mathfrak{su}}(2)_k$, the general expression (A.20) becomes

$$Z_{\alpha=j}(\tau) = \sum_{i=0}^{k/2} N_{jj}^i \, \chi_i(\tau). \tag{A.21}$$

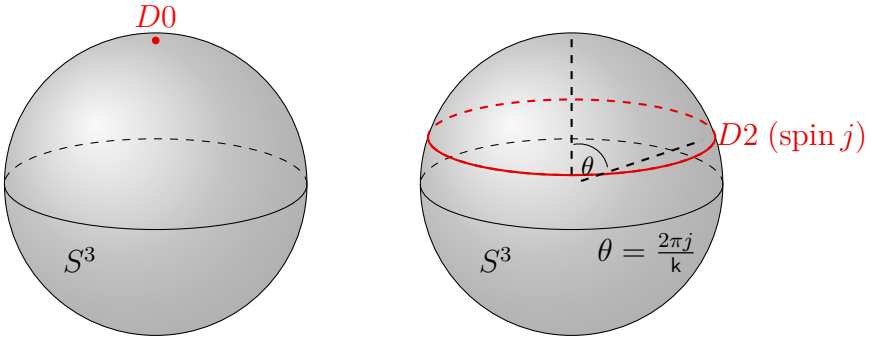

Figure 13: Left: D0-brane boundary condition. These correspond to spin $j = 0$ and $j = k/2$. Right: D2-brane boundary condition. These correspond to spin $j = 1/2, 1, \dots k$. This figure appeared before in [2]. (For interpretation of the references to color in this figure legend, the reader is referred to the web version of this article [https://jhap.du.ac.ir/].)

This is to be contrasted with (A.11). In string theory BCFT describes open strings, i.e. branes. In that context (A.20) (and thus (A.21)) count the field content on the worldvolume of a brane.

In general, a geometric interpretation can be assigned the boundary conditions of WZW models based on $\hat{\mathfrak{g}}_k$. WZW models are conformal field theories with group target, that is, they map the complex plane or the upper half plane into the group manifold G. In the case relevant in the Kondo model, this is $\mathrm{SU}(2) \simeq S^3$. Each boundary condition corresponds to one conjugacy class on SU(2). There are two distinct types of boundary conditions for SU(2)

Pointlike (D0) The conjugacy classes of the two center elements $\pm e$, with e the group unit. These are zero dimensional sets. We call these D0-branes because they occupy no spatial direction; they are zero-dimensional after all. Their spectrum is given by (A.21) with $j = 0$ for a $D0$-brane sitting at the north pole and $j = k/2$ for a $D0$-brane sitting at the south pole.

Spherical (D2) All other conjugacy classes are two-dimensional and known to coincide with two-spheres wrapping $\mathrm{SU}(2) \simeq S^3$. Once a Cartan torus is chosen, one still has half a $U(1)$'s worth of these conjugacy classes to choose from. We call these D2-branes, because they occupy two spatial directions. Their spectrum is given by (A.21) with $j \neq 0$ and $j \neq k/2$.

Now, the set of primaries and hence of conformal boundary conditions is finite. In contrast, SU(2) has a $U(1)$'s worth of conjugacy classes. Due to this mismatch not every conjugacy class can correspond to a boundary condition. In order to determine which conjugacy classes are eligible, we choose a Cartan torus on SU(2). This amounts to choosing spherical coordinates and, in particular, a polar angle $\theta \in [0, \pi]$. The north pole, $\theta = 0$, corresponds to the primary of the vacuum, $j = 0$, while the south pole, $\theta = \pi$, corresponds to $j = k/2$. Both are pointlike, i.e. $D0$-branes. The remaining $k - 1$ boundary conditions correspond to conjugacy classes, which are equally spaced on the polar angle $\theta = \frac{2\pi j}{k}$. This is illustrated in figure 13.

A.2.3 Boundary States

The data of each BCFT is captured elegantly in *boundary states* $\|\mathcal{B}\rangle\!\rangle$. The basis for their construction is (A.17). Via worldsheet duality this condition maps into an operator $(L_n - \overline{L}_{-n})$, which in turn defines the boundary states

$$(L_n - \overline{L}_{-n})\|\mathcal{B}\rangle\!\rangle = 0, \qquad n \in \mathbb{Z} \tag{A.22}$$

In accordance with the fact that there is one conformal boundary condition per primary, there is also one boundary state $\|\mathcal{B}\rangle\!\rangle$ per primary, at least for rational CFTs.

Extended symmetries, say Kac-Moody symmetries, are glued according to (A.19). Via worldsheet duality this maps into

$$(J_n + \Omega[\overline{J}_{-n}])\|\mathcal{B}\rangle\!\rangle = 0 \tag{A.23}$$

In this review, no explicit use boundary states is made, which is why we keep our discussion on boundary states at a minimum. Nevertheless, anybody who wishes to seriously work with BCFT should however take a closer look either at the original source [87, 88] or the reviews [59, 78, 85, 86]. For our purposes boundary states provide an excellent vantage point to introduce interfaces in CFT.

A.3 Interfaces in Conformal Field Theory

Interfaces provide mappings between theories through generalized boundary conditions. This turns them into rich playgrounds for a great host of ideas. For instance they are of interest when studying the interplay of (conformal) field theories [89–93], in holography [94–101], in impurity problems [102–107] and entanglement [108, 109]. The Kondo impurity, discussed in section 2, may in fact be seen as an interface between two chiral CFTs, and the Kondo effect as an interface RG flow. In this section we follow [94].

Folding Trick

Let us consider the tensor product of two possibly distinct CFTs, $\mathrm{CFT}_1 \otimes \mathrm{CFT}_2$ and we confine it to the upper half-plane, $\Im(z) \geq 0$, as we did when setting up a BCFT. What are the allowed boundary states of this new system? The formal answer is given by the analogue of (A.22),

$$(L_n^{(1)} + L_n^{(2)} - \overline{L}_{-n}^{(1)} - \overline{L}_{-n}^{(2)})\|\mathcal{B}\rangle\!\rangle = 0, \qquad n \in \mathbb{Z}, \tag{A.24}$$

where $L_n^{(i)}$ and $\overline{L}_n^{(i)}$ are the Virasoro modes of CFT_i, with $i = 1, 2$. Now comes a conceptual leap: CFT_2 is unfolded onto the lower half plane with $\Im(z) \leq 0$, as depicted in figure 14. The relative orientation of CFT_2 towards the boundary changes under this operation. To correct this, the holomorphic and antiholomorphic sectors have to be interchanged

$$\mathrm{CFT}_2 \to \overline{\mathrm{CFT}_2} \tag{A.25}$$

After this operation CFT_1 resides still on the upper half-plane, separated by the real line from $\overline{\mathrm{CFT}_2}$ on the lower half-plane; see figure 14. The separation line is called an *interface*. When $\mathrm{CFT}_1 = \mathrm{CFT}_2$, these are called *defects* rather than interfaces.

When working with a boundary on the real line, i.e. before unfolding, the condition (A.24) prohibits energy-momentum flow across the boundary. After unfolding it becomes

$$(L_n^{(1)} + \overline{L}_n^{(2)} - \overline{L}_{-n}^{(1)} - L_{-n}^{(2)})\|\mathcal{B}\rangle\!\rangle = 0, \qquad n \in \mathbb{Z}, \tag{A.26}$$

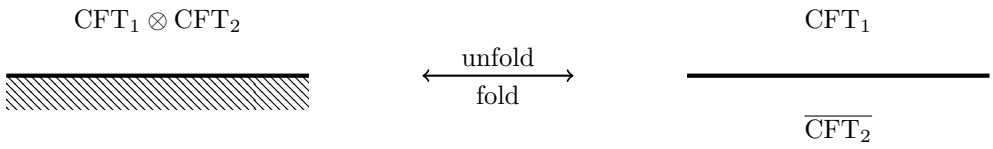

Figure 14: The BCFT of the combined system $\mathrm{CFT}_1 \otimes \mathrm{CFT}_2$ (left) is unfolded along the boundary into an interface theory between CFT_1 on the upper half-plane and $\overline{\mathrm{CFT}_2}$ on the lower half-plane (right). Similarly, interface theories can be folded along the interface into boundary theories. This figure appeared before in [2].

and its interpretation changes. It now implies continuity of $T - \overline{T}$ along the real line, with $T = T^{(1)} + T^{(2)}$ [94].

The next step is to analyze some solutions to (A.26). One possible solution is

$$\|\mathcal{B}\rangle\rangle_{\text{Reflect}} = \|\mathcal{B}_1\rangle\rangle \otimes \|\mathcal{B}_2\rangle\rangle. \tag{A.27}$$

Due to the factorization the operators $(L_n^{(1)} - \overline{L}_{-n}^{(1)})$ and $(\overline{L}_{-n}^{(1)} - L_n^{(2)})$ annihilate individually the boundary state $\|\mathcal{B}\rangle\rangle$. While the former is equivalent to (A.22) for the upper half-plane, the latter is too, but after application of (A.25). Therefore, there is no energy-momentum leakage across the interface. CFT_1 and CFT_2 do not communicate: they decouple. This is true, up to the subtlety that the boundary conditions on the lower half-plane and the upper half-plane may be correlated. Nevertheless, we speak of *factorizable* boundary states whenever (A.27) holds.

Another option is to have the interface simply glue $T^{(1)} = \overline{T}^{(2)}$ and $\overline{T}^{(1)} = T^{(2)}$ at $z = \overline{z}$. In the boundary theory this corresponds to $T^{(1)} = T^{(2)}$ and $\overline{T}^{(1)} = \overline{T}^{(2)}$ respectively. In the unfolded picture this corresponds to the operator relations

$$\left(L_n^{(1)} - \overline{L}_{-n}^{(2)}\right) \|\mathcal{B}\rangle\rangle_{\text{ transmit}} = 0 \tag{A.28}$$

$$\left(L_n^{(2)} - \overline{L}_{-n}^{(1)}\right) \|\mathcal{B}\rangle\rangle_{\text{ transmit}} = 0 \tag{A.29}$$

These interfaces are totally transmissive. The simplest case of this scenario occurs when $\mathrm{CFT}_1 = \mathrm{CFT}_2$. The theories must not be identical however. For instance, the upper theory could be a free scalar compactified at radius R, while the lower theory is again a free scalar, but now compactified at radius $r \neq R$.

Totally reflective boundary states, (A.27) and totally transmissive boundary states, (A.28), constitute the two extremes of possible boundary states for interfaces. Generic interfaces lie somewhere in between and are in general described by an entangled boundary state.

B Page Charges in Supergravity Solutions

In this appendix, the Page charges, which are employed in section 4, are described. An introduction is found in [109]. Page charges are conserved, localized and quantized. The first two properties allow to associate the correct amount of charge with points on Σ, corresponding either to the interface or CFT loci. The third property sets them into relation with the quantized number of one- and five-branes. Note that the Page charges are not gauge invariant. Full details on the derivation of the Page charges used this review are found in the appendix of [64]. Only the final expressions are collected here.

The D1-brane Page charge reads

$$Q_{D1} = -\int_{S^7}\Big(e^{\phi}\star\big(dC_{(2)}-\chi H_{(3)}\big)-C_{(4)}\wedge H_{(3)}\Big). \tag{B.1}$$

Due to the symmetry of the ansatz (4.1) the three-forms are organized according to

$$H_{(3)} = dB_{(2)} = (\partial_a b^{(1)})da\wedge\omega_{\mathrm{AdS}_2}+(\partial_a b^{(2)})da\wedge\omega_{S^2}, \tag{B.2a}$$
$$F_{(3)} = dC_{(2)} = (\partial_a c^{(1)})da\wedge\omega_{\mathrm{AdS}_2}+(\partial_a c^{(2)})da\wedge\omega_{S^2}, \tag{B.2b}$$

where $a=z,\bar z$ labels the coordinates on Σ. In terms of the harmonic functions (4.3), $b^{(i)}$ and $c^{(i)}$ are given by

$$b^{(1)} = -\frac{2v\,b}{a\,u-b^2}-h_1, \qquad h_1=\int\frac{\partial_z v}{B}+c.c., \tag{B.3a}$$
$$b^{(2)} = \frac{2v\,\tilde b}{a\,u+\tilde b^2}+\tilde h_1, \qquad \tilde h_1=\frac{1}{i}\int\frac{\partial_z v}{B}+c.c., \tag{B.3b}$$
$$c^{(1)} = -v\frac{a\,\tilde b-\tilde a\,b}{a\,u-b^2}+\tilde h_2, \qquad \tilde h_2=\frac{1}{i}\int A\frac{\partial_z v}{B}+c.c., \tag{B.3c}$$
$$c^{(2)} = -v\frac{a\,b+\tilde a\,\tilde b}{a\,u+\tilde b^2}+h_2, \qquad h_2=\int A\frac{\partial_z v}{B}+c.c. \tag{B.3d}$$

The Page one-brane charges are given by contour integrals

$$\begin{aligned}Q_{D1} = 4\pi\Big[&\int_{\mathcal{C}}\frac{u}{a}\frac{a\,u-b^2}{a\,u+\tilde b^2}\,i(\partial_z c^{(1)}-\chi\partial_z b^{(1)})dz\\ &+\int_{\mathcal{C}}C_K\partial_z b^{(2)}dz\Big]+c.c.\end{aligned} \tag{B.4a}$$

$$\begin{aligned}Q_{F1} = 4\pi\Big[&\int_{\mathcal{C}}\frac{(a\,u-b^2)^2}{4a\,u}i\partial_z b^{(1)}dz-\int C_K\partial_z c^{(2)}dz\\ &-\int_{\mathcal{C}}\frac{u}{a}\frac{a\,u-b^2}{a\,u+\tilde b^2}\,\chi\,i(\partial_z c^{(1)}-\chi\partial_z b^{(1)})dz\Big]+c.c.\,,\end{aligned} \tag{B.4b}$$

where the contour $\mathcal{C}$ is a semicircle anchored at the boundary $\partial\Sigma$. It arises from partitioning the integration domain in (B.1) as $S^7=T^4\times S^2\times\mathcal{C}$. The Page five-brane charges are[18]

$$Q_{NS5} = 4\pi\Big(\int_{\mathcal{C}}dz\,\partial_z b^{(2)}+c.c.\Big) \tag{B.5a}$$
$$Q_{D5} = 4\pi\Big(\int_{\mathcal{C}}dz\,\partial_z c^{(2)}+c.c.\Big). \tag{B.5b}$$

[18] While the one-brane charges are electric charges, the five-brane charges are magnetic.

Once again, the contour $\mathcal{C}$ is a semicircle anchored at $\partial\Sigma$ around poles on the boundary. Together with the fibered S^2, $\mathcal{C}$ yields an S^3, as is necessary to enclose a five-brane.

In analogy the Page D3-brane charge is given by

$$Q_{D3} = \oint_{\mathcal{C}} \left(\partial_z C_K \, dz + c.c. \right) \tag{B.6}$$

In this case, the contour $\mathcal{C}$ is given by an S^1, which together with T^4 gives a five manifold as required for the enclosure of a three-brane. In contrast to the previous charges, this contour encloses a point in the interior of Σ.

References

[1] J. Erdmenger, C. M. Melby-Thompson and C. Northe, "Holographic RG Flows for Kondo-like Impurities", JHEP **05**, 075 (2020).

[2] C. Northe, Interfaces and Information in Gauge/Gravity Duality, Ph.D. thesis, U. Wurzburg (main), 2019.

[3] J. Kondo, "Resistance Minimum in Dilute Magnetic Alloys", Progress of Theoretical Physics **32**, 37-49 (1964).

[4] K. G. Wilson, "The Renormalization Group: Critical Phenomena and the Kondo Problem", Rev. Mod. Phys. **47**, 773 (1975).

[5] P. Nozires, "A fermi liquid description of the kondo problem at low tempertures", Journal of Low Temperature Physics **17** 3142 (1974).

[6] N. Andrei, "Diagonalization of the Kondo Hamiltonian", Phys. Rev. Lett. **45**, 379 (1980).

[7] N. Andrei and C. Destri, "Solution of the Multichannel Kondo Problem", Phys. Rev. Lett. **52**, 364367 (1984).

[8] N. E. Bickers, "Review of techniques in the large-N expansion for dilute magnetic alloys", Rev. Mod. Phys. **59**, 845939 (1987).

[9] I. Affleck, "A Current Algebra Approach to the Kondo Effect", Nucl. Phys. B**336**, 517532 (1990).

[10] I. Affleck and A. W. Ludwig, "The kondo effect, conformal field theory and fusion rules", Nuclear Physics B **352**, 849 862 (1991).

[11] I. Affleck and A. W. Ludwig, "Critical theory of overscreened kondo fixed points", Nuclear Physics B **360**, 641 696 (1991).

[12] I. Affleck and A. W. W. Ludwig, "Universal noninteger ground state degeneracy' in critical quantum systems", Phys. Rev. Lett. **67**, 161164 (1991).

[13] I. Affleck and A. W. W. Ludwig, "Exact conformal-field-theory results on the multichannel kondo effect: Single-fermion greens function, self-energy, and resistivity", Phys. Rev. B **48**, 72977321 (1993).

[14] S. Fredenhagen and V. Schomerus, "Branes on group manifolds, gluon condensates, and twisted K theory", JHEP **04**, 007 (2001).

[15] S. Fredenhagen and V. Schomerus, "Brane dynamics in CFT backgrounds", in Strings 2001: International Conference Mumbai, India, January 5-10, 2001, 2001.

[16] S. Fredenhagen and V. Schomerus, "D-branes in coset models", JHEP **02**, 005 (2002).

[17] S. Fredenhagen and V. Schomerus, "On boundary RG flows in coset conformal field theories", Phys. Rev. D**67**, 085001 (2003).

[18] S. Fredenhagen, "Organizing boundary RG flows", Nucl. Phys. B**660**, 436472 (2003).

[19] A. Yu. Alekseev, S. Fredenhagen, T. Quella and V. Schomerus, "Noncommutative gauge theory of twisted D-branes", Nucl. Phys. B**646**, 127157 (2002).

[20] C. Bachas and M. Gaberdiel, "Loop operators and the Kondo problem", JHEP **11**, 065 (2004).

[21] M. Kormos, I. Runkel and G. M. T. Watts, "Defect flows in minimal models", JHEP **11**, 057 (2009).

[22] L. Kouwenhoven and L. Glazman, "Revival of the Kondo effect", arXiv e-prints (Apr, 2001) condmat/0104100, [cond-mat/0104100].

[23] M. A. Sierra, R. Lpez and J. S. Lim, "Thermally driven out-of-equilibrium two-impurity kondo system", Phys. Rev. Lett. **121**, 096801 (2018).

[24] M. A. Sierra and D. Snchez, Heat current through an artificial kondo impurity beyond linear response, Journal of Physics: Conference Series **969**, 012144 (2018).

[25] D. Bak, M. Gutperle and S. Hirano, "A Dilatonic deformation of AdS(5) and its field theory dual", JHEP **05**, 072 (2003).

[26] N. Bobev, K. Pilch and N. P. Warner, "Supersymmetric Janus Solutions in Four Dimensions", JHEP **06**, 058 (2014).

[27] M. Fujita, C. M. Melby-Thompson, R. Meyer and S. Sugimoto, "Holographic Chern-Simons Defects", JHEP **06**, 163 (2016).

[28] C. Melby-Thompson and C. Schmidt-Colinet, "Double Trace Interfaces", JHEP **11**, 110 (2017).

[29] P. Karndumri and K. Upathambhakul, "Supersymmetric RG flows and Janus from type II orbifold compactification", Eur. Phys. J. C**77**, 455 (2017).

[30] M. Fujita, R. Meyer, S. Pujari and M. Tezuka, "Effective Hopping in Holographic Bose and Fermi Hubbard Models", JHEP **01**, 045 (2019).

[31] N. Evans, A. O'Bannon and R. Rodgers, "Holographic Wilson Lines as Screened Impurities", JHEP **03**, 188 (2020).

[32] S. Harrison, S. Kachru and G. Torroba, "A maximally supersymmetric Kondo model", Class. Quant. Grav. **29**, 194005 (2012).

[33] J. Erdmenger, C. Hoyos, A. O'Bannon and J. Wu, "A Holographic Model of the Kondo Effect", JHEP **12**, 086 (2013).

[34] J. Erdmenger, M. Flory and M.-N. Newrzella, "Bending branes for DCFT in two dimensions", JHEP**01**, 058 (2015).

[35] A. OBannon, I. Papadimitriou and J. Probst, "A Holographic Two-Impurity Kondo Model", JHEP **01**, 103 (2016).

[36] J. Erdmenger, M. Flory, C. Hoyos, M.-N. Newrzella and J. M. S. Wu, "Entanglement Entropy in a Holographic Kondo Model", Fortsch. Phys. **64**, 109130 (2016).

[37] J. Erdmenger, M. Flory, C. Hoyos, M.-N. Newrzella, A. O'Bannon and J. Wu, "Holographic impurities and Kondo effect", Fortsch. Phys. **64**, 322329 (2016).

[38] J. Erdmenger, C. Hoyos, A. OBannon, I. Papadimitriou, J. Probst and J. M. S. Wu, "Holographic Kondo and Fano Resonances", Phys. Rev. D**96**, 021901 (2017).

[39] J. Erdmenger, C. Hoyos, A. O'Bannon, I. Papadimitriou, J. Probst and J. M. S. Wu, "Two-point Functions in a Holographic Kondo Model", JHEP **03**, 039 (2017).

[40] J. Erdmenger, M. Flory, M.-N. Newrzella, M. Strydom and J. M. S. Wu, "Quantum Quenches in a Holographic Kondo Model", JHEP **04**, 045 (2017).

[41] J. M. Luttinger, "An exactly soluble model of a many-fermion system", Journal of Mathematical Physics **4**, 11541162 (1963).

[42] A. Yu. Alekseev, A. Recknagel and V. Schomerus, "Brane dynamics in background fluxes and noncommutative geometry", JHEP **05**, 010 (2000).

[43] R. C. Myers, "Dielectric branes", JHEP **12**, 022 (1999).

[44] N. Seiberg and E. Witten, "The D1 / D5 system and singular CFT", JHEP **04**, 017 (1999).

[45] M. F. Atiyah, N. J. Hitchin, V. G. Drinfeld and Yu. I. Manin, "Construction of Instantons", Phys. Lett. A**65**, 185187 (1978).

[46] D. Tong and K. Wong, Instantons, Wilson lines, and D-branes, Phys. Rev. D**91**, 026007 (2015).

[47] I. Affleck and A. W. W. Ludwig, "Critical theory of overscreened Kondo fixed points", Nucl. Phys. B**360**, 641696 (1991).

[48] I. Affleck and A. W. W. Ludwig, "The Kondo effect, conformal field theory and fusion rules", Nucl. Phys. B**352**, 849862 (1991).

[49] M. Chiodaroli, M. Gutperle and D. Krym, "Half-BPS Solutions locally asymptotic to $AdS_3 \times S^3$ and interface conformal field theories", JHEP **02**, 066 (2010).

[50] I. Affleck and A. W. W. Ludwig, "Universal noninteger 'ground state degeneracy' in critical quantum systems", Phys. Rev. Lett. **67**, 161164 (1991).

[51] D. Friedan and A. Konechny, "On the boundary entropy of one-dimensional quantum systems at low temperature", Phys. Rev. Lett. **93**, 030402 (2004).

[52] H. Casini, I. S. Landea and G. Torroba, "The g-theorem and quantum information theory", JHEP **10**, 140 (2016).

[53] P. Calabrese and J. Cardy, "Entanglement entropy and conformal field theory", J. Phys. A**42**, 504005 (2009).

[54] S. Ryu and T. Takayanagi, "Holographic derivation of entanglement entropy from AdS/CFT", Phys. Rev. Lett. **96**, 181602 (2006).

[55] M. Chiodaroli, M. Gutperle and L.-Y. Hung, "Boundary entropy of supersymmetric Janus solutions", JHEP **09**, 082 (2010).

[56] I. Affleck, "Conformal field theory approach to the Kondo effect", Acta Phys. Polon. B**26**, 18691932 (1995).

[57] P. Di Francesco, P. Mathieu and D. Senechal, "Conformal Field Theory". Graduate Texts in Contemporary Physics. Springer-Verlag, New York, 1997, 10.1007/978-1-4612-2256-9.

[58] P. Goddard and D. I. Olive, "Kac-Moody and Virasoro Algebras in Relation to Quantum Physics", Int. J. Mod. Phys. A**1**, 303 (1986).

[59] A. Recknagel and V. Schomerus, "Boundary Conformal Field Theory and the World-sheet Approach to D-Branes". Cambridge Monographs on Mathematical Physics. Cambridge University Press, 2013, 10.1017/CBO9780511806476

[60] C. Bachas and M. Petropoulos, "Anti-de Sitter D-branes", JHEP **02**, 025 (2001).

[61] C. Bachas, M. R. Douglas and C. Schweigert, "Flux stabilization of D-branes", JHEP **05**, 048 (2000).

[62] J. M. Camino, A. Paredes and A. V. Ramallo, "Stable wrapped branes", JHEP **05**, 011 (2001).

[63] T. Quella, I. Runkel and G. M. T. Watts, "Reflection and transmission for conformal defects", JHEP **04**, 095 (2007).

[64] M. Chiodaroli, M. Gutperle, L.-Y. Hung and D. Krym, "String Junctions and Holographic Interfaces", Phys. Rev. D**83**, 026003 (2011).

[65] M. Meineri, J. Penedones and A. Rousset, "Colliders and conformal interfaces", JHEP **02**, 138 (2020).

[66] L. Eberhardt, M. R. Gaberdiel, R. Gopakumar and W. Li, "BPS spectrum on $AdS_3 \times S^3 \times S^3 \times S^1$", JHEP **03**, 124 (2017).

[67] L. Eberhardt, M. R. Gaberdiel and W. Li, "A holographic dual for string theory on $AdS_3 \times S^3 \times S^3 \times S^1$", JHEP **08**, 111 (2017).

[68] S. Datta, L. Eberhardt and M. R. Gaberdiel, "Stringy N = (2, 2) holography for AdS_3", JHEP **01**, 146 (2018).

[69] L. Eberhardt, "Supersymmetric AdS_3 supergravity backgrounds and holography", JHEP **02**, 087 (2018).

[70] L. Eberhardt, M. R. Gaberdiel and I. Rienacker, "Higher spin algebras and large N = 4 holography", JHEP **03**, 097 (2018).

[71] L. Eberhardt and I. G. Zadeh, "N = (3, 3) holography on $AdS_3 \times (S^3 \times S^3 \times S^1)/Z2$, JHEP **07**, 143 (2018).

[72] L. Eberhardt and K. Ferreira, "The plane-wave spectrum from the worldsheet", JHEP **10**, 109 (2018).

[73] L. Eberhardt and K. Ferreira, "Long strings and chiral primaries in the hybrid formalism", JHEP **02**, 098 (2019).

[74] L. Eberhardt, M. R. Gaberdiel and R. Gopakumar, "The Worldsheet Dual of the Symmetric Product CFT", JHEP **04**, 103 (2019).

[75] L. Eberhardt and M. R. Gaberdiel, "String theory on AdS_3 and the symmetric orbifold of Liouville theory", Nucl.Phys.B **948**, 114774 (2019).

[76] L. Eberhardt and M. R. Gaberdiel, "Strings on $AdS_3 \times S^3 \times S^3 \times S^1$", JHEP **06**, 035 (2019).

[77] A. Dei, L. Eberhardt and M. R. Gaberdiel, "Three-point functions in AdS3/CFT2 holography", JHEP **12**, 012 (2019).

[78] R. Blumenhagen and E. Plauschinn, "Introduction to Conformal Field Theory: With Applications to String Theory". Lecture Notes in Physics 779. Springer, Berlin Heidelberg, 2009.

[79] P. H. Ginsparg, "Applied Conformal Field Theory", in Les Houches Summer School in Theoretical Physics: Fields, Strings, Critical Phenomena Les Houches, France, June 28-August 5, 1988, pp. 1168, 1988.

[80] K. Gawedzki, "Conformal field theory: A Case study", [Arxiv: hep-th/9904145].

[81] E. Witten, "Nonabelian Bosonization in Two-Dimensions", Commun. Math. Phys. **92**, 455472 (1984).

[82] G. W. Moore and N. Seiberg, "Polynomial Equations for Rational Conformal Field Theories", Phys. Lett. B**212**, 451460 (1988).

[83] M. Gaberdiel, "Fusion in conformal field theory as the tensor product of the symmetry algebra", Int. J. Mod. Phys. A**9**, 46194636 (1994).

[84] J. L. Cardy, "Boundary Conditions, Fusion Rules and the Verlinde Formula", Nucl. Phys. B**324**, 581596 (1989).

[85] J. L. Cardy, "Conformal Invariance and Statistical Mechanics", in Les Houches Summer School in Theoretical Physics: Fields, Strings, Critical Phenomena Les Houches, France, June 28-August 5, 1988, pp. 0169246, 1989.

[86] M. R. Gaberdiel, "Boundary conformal field theory and d-branes, Lectures given at the TMR network school on Nonperturbative methods in low dimensional integrable models", Budapest 1521 (2003).

[87] N. Ishibashi, "The Boundary and Crosscap States in Conformal Field Theories", Mod. Phys. Lett. A**4**, 251 (1989).

[88] T. Onogi and N. Ishibashi, "Conformal Field Theories on Surfaces With Boundaries and Crosscaps", Mod. Phys. Lett. A**4**, 161 (1989).

[89] R. E. Behrend, P. A. Pearce, V. B. Petkova and J.-B. Zuber, "Boundary conditions in rational conformal field theories", Nucl. Phys. B**570**, 525589 (2000).

[90] V. B. Petkova and J. B. Zuber, "Generalized twisted partition functions", Phys. Lett. B**504**, 157164 (2001).

[91] J. Frohlich, J. Fuchs, I. Runkel and C. Schweigert, "Duality and defects in rational conformal field theory", Nucl. Phys. B**763**, 354430 (2007).

[92] I. Brunner, N. Carqueville and D. Plencner, "A quick guide to defect orbifolds", Proc. Symp. Pure Math. **88**, 231242 (2014).

[93] C. Bachas, I. Brunner and D. Roggenkamp, "Fusion of Critical Defect Lines in the 2D Ising Model", J. Stat. Mech. **1308**, P08008 (2013).

[94] C. Bachas, J. de Boer, R. Dijkgraaf and H. Ooguri, "Permeable conformal walls and holography", JHEP **06**, 027 (2002).

[95] A. Karch and L. Randall, "Open and closed string interpretation of SUSY CFTs on branes with boundaries", JHEP **06**, 063 (2001).

[96] O. DeWolfe, D. Z. Freedman and H. Ooguri, "Holography and defect conformal field theories", Phys. Rev. D**66**, 025009 (2002).

[97] J. Erdmenger, Z. Guralnik and I. Kirsch, "Four-dimensional superconformal theories with interacting boundaries or defects", Phys. Rev. D**66**, 025020 (2002).

[98] O. Aharony, O. DeWolfe, D. Z. Freedman and A. Karch, "Defect conformal field theory and locally localized gravity", JHEP **07**, 030 (2003).

[99] A. Karch, J. Sully, C. F. Uhlemann and D. G. E. Walker, "Boundary Kinematic Space", JHEP **08**, 039 (2017).

[100] M. Bill, V. Goncalves, E. Lauria and M. Meineri, "Defects in conformal field theory", JHEP **04**, 091 (2016).

[101] S. Sachdev, C. Buragohain and M. Vojta, "Quantum Impurity in a Nearly Critical Two Dimensional Antiferromagnet", Science **286**, 2479 (1999).

[102] A. Kolezhuk, S. Sachdev, R. R. Biswas and P. Chen, "Theory of quantum impurities in spin liquids", Physical Review B **74**, 165114 (2006).

[103] S. Powell and S. Sachdev, "Excited-state spectra at the superfluid-insulator transition out of paired condensates", Physical Review A **75**, 031601 (2007).

[104] S. Powell and S. Sachdev, "Spin dynamics across the superfluid-insulator transition of spinful bosons", Physical Review A **76**, 033612 (2007).

[105] M. A. Metlitski and S. Sachdev, "Valence bond solid order near impurities in two-dimensional quantum antiferromagnets", Physical Review B **77**, 054411 (2008).

[106] A. Allais and S. Sachdev, "Spectral function of a localized fermion coupled to the Wilson-Fisher conformal field theory", Phys. Rev. B**90**, 035131 (2014).

[107] L. Bianchi, M. Meineri, R. C. Myers and M. Smolkin, "Rnyi entropy and conformal defects", JHEP **07**, 076 (2016).

[108] E. M. Brehm, I. Brunner, D. Jaud and C. Schmidt-Colinet, "Entanglement and topological interfaces", Fortsch. Phys. **64**, 516535 (2016).

[109] D. Marolf, "Chern-Simons terms and the three notions of charge, in Quantization, gauge theory, and strings". Proceedings, International Conference dedicated to the memory of Professor Efim Fradkin, Moscow, Russia, June 5-10, 2000. Vol. 1+2, pp. 312320, 2000, [Arxiv:hep-th/0006117].